

## Article

# Novel Synchronization Criteria for Non-Dissipative Coupled Networks with Bounded Disturbances and Time-Varying Delays of Unidentified Bounds via Impulsive Sampling Control

Hongguang Fan <sup>1,2,3</sup> , Kaibo Shi <sup>4</sup> , Yanan Xu <sup>1</sup>, Rui Zhang <sup>1</sup>, Shuai Zhou <sup>1</sup> and Hui Wen <sup>2,5,\*</sup> 

- <sup>1</sup> College of Computer, Chengdu University, Chengdu 610106, China; fanhongguang@cdu.edu.cn (H.F.)
- <sup>2</sup> Engineering Research Center of Big Data Application in Private Health Medicine, Fujian Province University, Putian 351100, China
- <sup>3</sup> School of Mathematical and Computational Science, Hunan University of Science and Technology, Xiangtan 411201, China
- <sup>4</sup> School of Electronic Information and Electrical Engineering, Chengdu University, Chengdu 610106, China
- <sup>5</sup> New Engineering Industry College, Putian University, Putian 351100, China
- \* Correspondence: wen\_hui81@163.com

**Abstract:** The  $\mu$ -synchronization issues of non-dissipative coupled networks with bounded disturbances and mixed delays are studied in this article. Different from existing works, three kinds of time delays, including internal delays, coupling delays, and impulsive sampling delays, have unidentified bounds and even evolve towards infinity over time, making the concerned network more practical. Considering  $\mu$ -stability theory and impulse inequality techniques, a hybrid non-delayed and time-delayed impulsive controller including both current and historical state information is designed, and several novel sufficient conditions are derived to make nonlinear complex networks achieve  $\mu$ -synchronization. Moreover, not only can the constriction of dissipative coupling conditions on network topology be relaxed, but also the restriction of various time delays on impulsive intervals can be weakened, which makes the theoretical achievements in this article more general than the previous achievements. Ultimately, numerical simulations confirm the effectiveness of our results.



**Citation:** Fan, H.; Shi, K.; Xu, Y.; Zhang, R.; Zhou, S.; Wen, H. Novel Synchronization Criteria for Non-Dissipative Coupled Networks with Bounded Disturbances and Time-Varying Delays of Unidentified Bounds via Impulsive Sampling Control. *Electronics* **2023**, *12*, 4175. <https://doi.org/10.3390/electronics12194175>

Academic Editor: Nikolay Hinov

Received: 27 August 2023

Revised: 6 October 2023

Accepted: 7 October 2023

Published: 8 October 2023



**Copyright:** © 2023 by the authors. Licensee MDPI, Basel, Switzerland. This article is an open access article distributed under the terms and conditions of the Creative Commons Attribution (CC BY) license (<https://creativecommons.org/licenses/by/4.0/>).

**Keywords:** dynamical network; Lyapunov function; synchronization condition; stability analysis; topological structure

## 1. Introduction

Recently, complex dynamic networks have received increasing attention by reason of their important applications in intelligent identification, automatic processing, system stability, etc. For instance, complex networks can be used for information protection, such as image encryption [1] and secure communication [2]. Random neural networks can be used for general dissipativity analysis [3] and extended dissipativity analysis [4]. Combining DOS attacks and complex networks, image protection methods [5] and system stability conditions [6] can be obtained. By utilizing machine learning rules for complex dynamic networks, trajectory tracking can be achieved in [7]. Among the various aggregation behaviors of complex networks, synchronization undoubtedly becomes one of the most prominent dynamical evolution statuses [8]. Considering the complexity of network structures and the interactive influence between different nodes, utilizing external forces to achieve network synchronization is the most common strategy. Presently, various control technologies, including but not limited to predictive control [9], tracking control [10], intermittent control [11], linear control [12], and impulsive control [13], have been utilized in the synchronization research of neural networks or complex dynamical networks.

As a typical discrete control method, impulsive control only applies external forces to the controlled system at a small number of impulse moments, effectively downgrading control duration and enhancing communication security [14]. The above distinguishing

features of impulsive control are widely favored by researchers, and a large number of synchronous research achievements on complex networks have been gained from this control mechanism. For example, Deng et al. [15] explored the impulsive synchronization for a kind of linearly-coupled group network through transient information interchange at part-discrete impulse instants. Peng et al. [16] paid attention to the asymptotic synchronization of drive–response complex systems by activating the sensor at event-triggered instants. Yang et al. [17] acquired sufficient synchronization conditions for uncertain switching of complex networks based on convex combination strategies and impulsive sampling control schemes. The above synchronization results involving impulsive mechanisms are interesting and valuable, but, regrettably, any time delay was not taken into account. As is well known, time delays are commonly present in actual network systems because of finite communication channel width and signal transfer rate. When studying the dynamical behavior of networks, ignoring the important factor of time delays may lead to imprecise or false results [18]. In [19], some important criteria were derived that ensure the admissibility of a type of singular system with state delays. In [20], Kchaou et al. obtained several sufficient requirements to ensure that the sliding mode dynamics of nonlinear systems were robust and tolerable. Constant time delays in couplings and dynamics have been explored in [21], and impulsive synchronization conditions for coupled networks including fractional order have been derived via mixed impulsive control methods. In [22], Yang et al. introduced time-varying internal delays to switching networks and obtained some important synchronization criteria for considering models by applying impulsive control. Feng et al. explored asymptotic synchronization [23] and exponential synchronization [24] for a type of coupled complex network including variable internal delays and coupling delays, and these two kinds of delays satisfied  $0 \leq \tau_1(t) \leq \tau_1, 0 \leq \tau_2(t) \leq \tau_2$ . It is noteworthy that these research results obtained above assume that internal or coupling delays have known or estimable boundaries.

In addition to the internal time delays and coupling time delays mentioned above, the sampling time delays in impulsive control processes also need to be attention. Due to limited sampling and transmission rates, it is hard to promptly accomplish the sampling, processing, and transmission of impulse signals at certain impulsive points, which inevitably results in sampling delays at impulsive instants. Some scholars have paid attention to this phenomenon and obtained partial relevant results based on time-delayed impulsive control frameworks. For instance, Ye et al. [25] designed an impulsive controller including impulse delays for coupled neural networks with fractional unmeasured information and obtained some helpful lag synchronization conditions. Liu et al. [26] discussed the global synchronization of linear complex dynamic systems by considering the time delays' positive or negative influence on the impulsive control mechanism. The authors in [27] deliberated on the asymptotic synchronization of fuzzy dynamic networks with random disturbances via a time-delayed impulsive controller. In [28], Wu et al. derived exponential synchronization criteria of random dynamical networks with reaction–diffusion items by using delayed impulsive control. More stability conditions [29] and synchronization results [30] stemming from impulsive control schemes with sampling delays can be found. However, the previous works assume that the bound of time delays in impulsive controllers is known or estimable, or even a constant. Under the constraints of these assumptions, no matter how the network evolves, the delay signal in the impulsive controller must be transmitted to controlled systems within a finite specified time. Actually, in addition to internal delays and coupling delays, the boundary of time delays of impulsive signals in impulsive controllers is also difficult to predict, even infinite. Hence, when we apply delayed impulsive control to solve synchronization challenges of complex networks involving variable delays, removing the boundedness assumptions of internal, coupling, and impulsive delays can obtain more practical and valuable synchronization results.

To handle the unpredictability and unidentified bounds of time delays, the  $\mu$ –function and the concept of  $\mu$ –stability were considered in [31].  $\mu$ –stability, as a generalized stability theory, can be applied to complex networks with unpredictable delays because the

historical information and current communication of nodes in the networks can be linked by  $\mu$ -function [32]. Cui et al. [33] attained the  $\mu$ -stability conditions for complex dynamical systems, including bounded distributed delays and internal delays of unknown bounds. Liu et al. [34] explored the  $\mu$ -stability issue of random complex networks involving unbounded internal delays. Chen et al. [35] popularized constant delays in complex network models to time-varying delays of unidentified bounds through certain mild conditions. The authors in [36] dealt with synchronization challenges of neural networks with unbounded system delays and coupling delays by establishing special  $\mu$ -functions. Additionally, uncertain bounded disturbances exist widely in the process of information interchange in various dynamical systems. For instance, Huang et al. [37] explored the synchronization requirements of complex networks under perturbations or non-perturbations in fixed time. Kaviarasa et al. analyzed the impact of uncertain internal coupling on the synchronization of neural networks in [38]. In [39], some synchronization conditions for dynamical networks with uncertain disturbances were studied by using adaptive control methods. Narayana et al. studied the impulsive control schemes for multi-agent systems under uncertain disturbances and attacks in [40]. For the sake of better simulation, various unpredictable time delays and uncertain norm-bounded disturbances need to be considered in the studies of synchronization. However, few or no works pay attention to the  $\mu$ -synchronization of complex networks involving bounded disturbances and mixed variable delays of unidentified bounds by hybrid non-delayed and time-delayed impulsive control, especially the boundary of impulsive delay is unidentified and unpredictable, which is the main motivation of this study.

Inspired by the above research achievements and utilizing non-delayed and delayed impulsive controllers, this article discusses  $\mu$ -synchronization for nonlinear complex networks, including bounded disturbances and mixed variable delays of unidentified bounds, and reveals the relationship between  $\mu$ -synchronization and other synchronization patterns, such as power synchronization, log synchronization, and exponential synchronization. The key highlights can be listed as follows. (1) To obtain more practical synchronization results, this paper focuses on a class of nonlinear dynamical networks that include bounded disturbances, internal delays, coupling delays, and sampling delays. In particular, all the delays considered in this study can be time-varying, non-differential, and unidentified bounds, which make the investigated model more generalized than the models with bounded delays in [18–24]. (2) The constriction of zero-row-sum conditions or dissipative coupling conditions on network topology can be relaxed, and the restriction of various time delays on impulsive intervals can also be weakened. (3) Different from existing control schemes [25–30], both non-delayed impulses and delayed impulses of unidentified bounds are considered concurrently in the impulsive controller, which implies information interchange between different nodes, including both current information and historical status information. Novel synchronization criteria for the concerned nonlinearly-coupled networks are derived under the hybrid non-delayed and delayed impulsive impacts.

## 2. Mathematical Model and Prior Knowledge

### 2.1. Notation Description

We first give the following set description. Set  $\Lambda_1 \subseteq R$ ,  $\Lambda_2 \subseteq R^k$ ,  $1 \leq k \leq n$ ,  $C^1(\Lambda_1, \Lambda_2) = \{v : \Lambda_1 \rightarrow \Lambda_2, v \text{ is continuously differentiable}\}$ .  $PC(\Lambda_1, \Lambda_2) = \{v : \Lambda_1 \rightarrow \Lambda_2, v \text{ is piecewise continuous except for a small number of points } t \text{ with } v(t^+) = v(t), \text{ and } v(t^-) \text{ exists}\}$ .  $PCB_\tau = \{\bar{v} \in PC([-\tau, 0], R^n), \bar{v} \text{ is bounded}\}$ , and the norm is computed by  $|\bar{v}| = \sup_{-\tau \leq s \leq 0} \|\bar{v}(s)\|$ .  $\aleph = \{\mu(t) \in C^1(R_+, [1, +\infty)) : \mu(t) \text{ is nondecreasing on } [0, +\infty) \text{ and } \mu(t) \rightarrow \infty \text{ as } t \rightarrow \infty\}$ . More mathematical symbols in master and slave networks can be seen in Table 1.

**Table 1.** Mathematical symbols utilized in this article.

$\lambda_{max}(A)$	The maximum eigenvalue of a matrix $A$ .
$u_i(t)$	The state vector of master networks.
$v_i(t)$	The state vector of slave networks.
$e_i(t)$	The error vector between master and slave networks.
$\beta(\cdot)$	The activation function of non-delayed parts.
$\gamma(\cdot)$	The activation function of delayed parts.
$\psi(\cdot)$	The coupling function of master and slave networks.
$\mathfrak{D}, \mathfrak{E}, \mathfrak{F}$	The connection synaptic matrices.
$\Delta\mathfrak{D}(t), \Delta\mathfrak{E}(t)$	The norm-bounded disturbances of non-delayed parts.
$\Delta\mathfrak{F}(t)$	The norm-bounded disturbances of delayed parts.
$\phi_i(t), \varphi_i(t)$	The initial conditions of master and slave networks.
$a_{ik}, c_{ik}$	The non-delayed and delayed impulsive strengths.
$B$	The coupling matrix.
$I$	The identity matrix.
$\eta_k$	The impulsive sampling delay.
$\tau_1(t)$	The internal time-varying delay.
$\tau_2(t)$	The coupling time-varying delay.

2.2. Model Description

Consider a nonlinear complex network including  $N$  nodes with delays of unidentified bounds as follows:

$$\begin{cases} \dot{u}_i(t) = -(\mathfrak{D} + \Delta\mathfrak{D}(t))u_i(t) + (\mathfrak{E} + \Delta\mathfrak{E}(t))\beta(u_i(t)) + (\mathfrak{F} + \Delta\mathfrak{F}(t))\gamma(u_i(t - \tau_1(t))) \\ \quad + \epsilon \sum_{j=1}^N b_{ij}\psi(u_j(t - \tau_2(t))), \\ u_i(s) = \phi_i(s), s \in (-\infty, 0], \end{cases} \tag{1}$$

where  $i = 1, 2, \dots, N$ , and  $u_i(t) = (u_{1i}(t), u_{2i}(t), \dots, u_{ni}(t))^T \in R^n$  denotes the state vector.  $\mathfrak{D}$  is a diagonal matrix with positive elements  $d_1, d_2, \dots, d_n$ .  $\mathfrak{E} \in R^{n \times n}$  and  $\mathfrak{F} \in R^{n \times n}$  represent the connection synaptic matrices.  $\Delta\mathfrak{D}(t) \in R^{n \times n}$ ,  $\Delta\mathfrak{E}(t) \in R^{n \times n}$ , and  $\Delta\mathfrak{F}(t) \in R^{n \times n}$  represent the norm-bounded disturbances, which are uncertain and time-varying.  $\beta(\cdot) \in R^n$  and  $\gamma(\cdot) \in R^n$  represent the nonlinear activation functions, and  $\psi(\cdot) \in R^n$  represents the nonlinear coupling function.  $\epsilon > 0$  stands for the coupling strength.  $\tau_1(t)$  and  $\tau_2(t)$  are the internal delay and the coupling delay, which are time-varying and have unidentified bounds, namely,  $0 \leq \tau_1(t) \leq \infty, 0 \leq \tau_2(t) \leq \infty$ .  $\phi_i(\cdot) \in PCB_\tau$  denotes the initial condition of node  $i$ .  $B = (b_{ij}) \in R^{N \times N}$  denotes the outer coupling matrix, where  $b_{ij}$  is defined as follows: if there exists an edge from node  $i$  to node  $j$  ( $i \neq j$ ), then  $b_{ij} > 0$ ; otherwise,  $b_{ij} = 0$ .

Taking the nonlinear dynamical network (1) as the master network, then the corresponding slave network could be given as:

$$\begin{cases} \dot{v}_i(t) = -(\mathfrak{D} + \Delta\mathfrak{D}(t))v_i(t) + (\mathfrak{E} + \Delta\mathfrak{E}(t))\beta(v_i(t)) + (\mathfrak{F} + \Delta\mathfrak{F}(t))\gamma(v_i(t - \tau_1(t))) \\ \quad + \epsilon \sum_{j=1}^N b_{ij}\psi(v_j(t - \tau_2(t))), t \neq t_k, \\ \Delta e_i(t_k) = a_{ik}e_i(t_k^-) + c_{ik}e_i(t_k^- - \eta_k), t = t_k, k \in Z_+, \\ v_i(s) = \varphi_i(s), s \in (-\infty, 0], \end{cases} \tag{2}$$

where  $v_i(t) = (v_{1i}(t), v_{2i}(t), \dots, v_{ni}(t))^T \in R^n$  is the state vector of response network (2).  $\varphi_i(\cdot) \in PCB_\tau$  represents the starting condition of node  $i$ . The impulsive equation

$$\Delta e_i(t_k) = a_{ik}e_i(t_k^-) + c_{ik}e_i(t_k^- - \eta_k), t = t_k, k \in Z_+, \tag{3}$$

denotes the hybrid non-delayed and time-delayed impulsive controller applied to the slave network, where  $e_i(\cdot) = v_i(\cdot) - u_i(\cdot)$  denotes the synchronization error of node  $i$ .

$\Delta e_i(t_k) = e_i(t_k^+) - e_i(t_k^-)$ , and this study assumes that  $e_i(t)$  is right-hand continuous, i.e.,  $e_i(t_k) = e_i(t_k^+)$ . The time sequences  $\{t_k, k \in \mathbb{Z}_+\}$  satisfy  $0 = t_0 < t_1 < \dots < t_k < \dots$  and  $t_k \rightarrow \infty$  as  $k \rightarrow \infty$ , and the set of impulsive sequences can be denoted by  $\mathcal{F}_0$ . For all  $\xi > 0$ , let  $\mathcal{F}(\xi) = \{t_k \in \mathcal{F}_0 | t_k - t_{k-1} \leq \xi, k \in \mathbb{Z}_+\}$ .  $\eta_k$  represents the impulsive sampling delay, which satisfies  $0 \leq \eta_k \leq \infty, k \in \mathbb{Z}_+$ . That is to say, the delay in the impulsive controller can also be an unidentified bound.  $a_{ik}$  and  $c_{ik}$  denote impulsive strengths at instants  $t_k$  and  $t_k - \eta_k$ , respectively. The nodes in master–slave networks are one-to-one correspondences, as seen in Figure 1. The top layer is the master network, and the bottom layer is the slave network. A dotted line denotes a directed link from a node in the master networks to the node in the slave networks. Each network consists of N-coupled nodes that are described by dynamical systems.

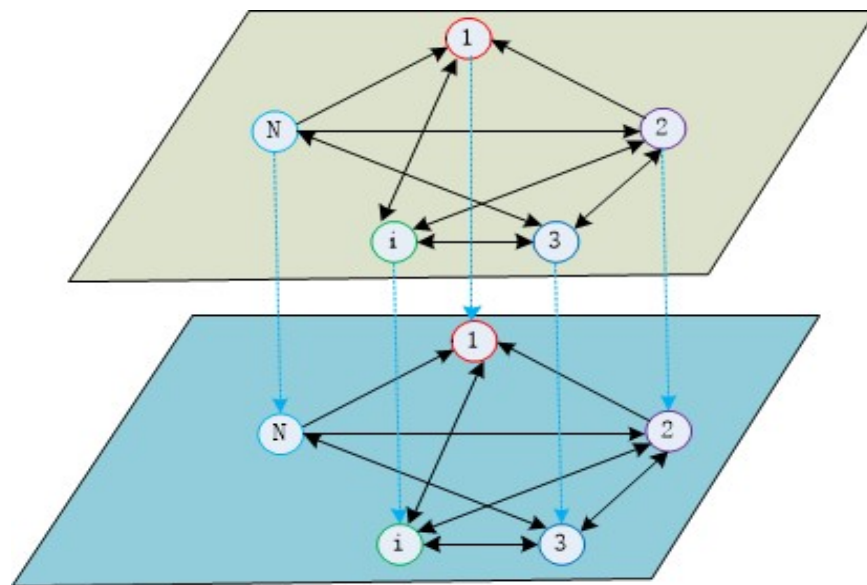


**Figure 1.** Master–slave networks consist of coupled dynamical networks.

**Remark 1.** There is not enough prior information about the boundary of time delays in most cases. In practical networks, for instance, in communication systems or power grids, time delays are affected by the transmission medium, sudden changes, and outer perturbation, which means the upper bound of delays cannot be precisely predicted. To establish a more generalized model, three different types of time delays are also introduced into the network apart from nonlinear coupling and bounded disturbances. Significantly, all delays can be time-varying, non-differentiable, and have unidentified bounds.

**Remark 2.** To obtain general synchronization criteria, in coupled complex networks, it is commonly supposed that the coupling topology matrix satisfies the zero-row-sum condition or dissipative coupling condition, such as [4,15–17,32]. This article removes this restrictive assumption, making the obtained synchronization criterion more practical.

**Remark 3.** Impulsive control intervals rely on the bound of time delays in existing research achievements, such as [12,13,29]. That is, as the time evolution and time delays increase, the impulse interval must be correspondingly reduced to ensure that the controlled systems attain a synchronization state. In this study, no matter how the time delays increase or if they have no upper bound, the synchronization objective can be fulfilled through given impulse intervals.

Combining master network (1) and slave network (2), one can derive the error system as follows:

$$\begin{cases} \dot{e}_i(t) = -(\mathfrak{D} + \Delta\mathfrak{D}(t))e_i(t) + (\mathfrak{E} + \Delta\mathfrak{E}(t))\bar{\beta}(e_i(t)) + (\mathfrak{F} + \Delta\mathfrak{F}(t))\bar{\gamma}(e_i(t - \tau_1(t))) \\ \quad + \epsilon \sum_{j=1}^N b_{ij}\bar{\psi}(e_j(t - \tau_2(t))), \quad t \neq t_k, \\ \Delta e_i(t_k) = a_{ik}e_i(t_k^-) + c_{ik}e_i(t_k^- - \eta_k), \quad t = t_k, \quad k \in Z_+, \\ e_i(s) = \varphi_i(s) - \phi_i(s), \quad s \in (-\infty, 0], \end{cases} \tag{4}$$

for  $i = 1, 2, \dots, N$ , where  $\bar{\beta}(e_i(t)) = \beta(v_i(t)) - \beta(u_i(t))$ ,  $\bar{\gamma}(e_i(t - \tau_1(t))) = \gamma(v_i(t - \tau_1(t))) - \gamma(u_i(t - \tau_1(t)))$  and  $\bar{\psi}(e_j(t - \tau_2(t))) = \psi(v_j(t - \tau_2(t))) - \psi(u_j(t - \tau_2(t)))$ . After that, the  $\mu$ -synchronization problem between the slave system (2) and the master system (1) can be transformed into the  $\mu$ -stability problem of the error system (4).

**Definition 1 ([35]).** Master–slave dynamical networks (1) and (2) are referred to as global  $\mu$ -synchronization, if one can find suitable  $\mu(t) \in \mathfrak{N}$  and  $\chi > 0$ , making the following inequality hold:

$$\|e_i(t)\| \leq \frac{\chi}{\mu(t)}, \quad t \geq 0, \quad i = 1, 2, \dots, N.$$

**Remark 4.** If the concrete mathematical expression of  $\mu$ -function is given, the equivalence between  $\mu$ -synchronization and the current mainstream synchronization pattern can be easily discovered. For instance, assuming  $\mu(t) = (1 + p_1t)^{p_2}$ ,  $p_1 > 0$ ,  $p_2 > 0$ ,  $\mu$ -synchronization can convert to power synchronization; assuming  $\mu(t) = \ln(e + q_1t)$ ,  $q_1 > 0$ ,  $\mu$ -synchronization can turn into log synchronization; considering  $\mu(t) = \exp(\omega t)$ ,  $\omega > 0$ ,  $\mu$ -synchronization can change into exponential synchronization.

**Assumption 1.** For activation functions  $\beta(\cdot)$ ,  $\gamma(\cdot)$  and nonlinear coupling function  $\psi(\cdot)$ , there exist three positive scalars,  $L_\beta$ ,  $L_\gamma$ , and  $L_\psi$ , such that

$$\|\beta(\eta) - \beta(\theta)\| \leq L_\beta\|\eta - \theta\|, \quad \|\gamma(\eta) - \gamma(\theta)\| \leq L_\gamma\|\eta - \theta\|, \quad \|\psi(\eta) - \psi(\theta)\| \leq L_\psi\|\eta - \theta\|$$

hold for any  $\eta, \theta \in R^n$ .

**Assumption 2.** The bounded disturbances  $\Delta\mathfrak{D}(t)$ ,  $\Delta\mathfrak{E}(t)$ , and  $\Delta\mathfrak{F}(t)$  can be described as

$$\Delta\mathfrak{D}(t) = G_{\mathfrak{D}}\Omega(t)H_{\mathfrak{D}}, \quad \Delta\mathfrak{E}(t) = G_{\mathfrak{E}}\Omega(t)H_{\mathfrak{E}}, \quad \Delta\mathfrak{F}(t) = G_{\mathfrak{F}}\Omega(t)H_{\mathfrak{F}},$$

where  $G_{\mathfrak{D}}, G_{\mathfrak{E}}, G_{\mathfrak{F}}, H_{\mathfrak{D}}, H_{\mathfrak{E}}, H_{\mathfrak{F}}$  represent known constant matrices and  $\Omega(t)$  denotes the unknown matrix satisfying the condition  $\Omega^T(t)\Omega(t) \leq I$ .

**Assumption 3.** For the outer coupling matrix  $B$ , there exists a scalar  $M_b > 0$  such that

$$\sum_{j=1}^N (b_{ij})^2 \leq M_b, \quad i = 1, 2, \dots, N.$$

**Assumption 4.** There exist constants  $\mu_i \geq 1$  ( $i = 0, 1, 2, 3$ ) such that  $\mu(t) \in \mathfrak{N}$  satisfies the conditions below:

$$\frac{\mu(t_k)}{\mu(t_{k-1})} \leq \mu_0, \quad \frac{\mu(t)}{\mu^*(t - \tau_1(t))} \leq \mu_1, \quad \frac{\mu(t)}{\mu^*(t - \tau_2(t))} \leq \mu_2, \quad \frac{\mu(t_k)}{\mu^*(t_k - \eta_k)} \leq \mu_3,$$

where  $k \in Z_+$ ,  $\mu^*(t) = \mu(t)$  when  $t \geq 0$ , and  $\mu^*(t) = 1$  when  $t < 0$ .



**Proof.** Choose the Lyapunov function below:

$$V(t) = \sum_{i=1}^N e_i^T(t) P e_i(t). \tag{9}$$

When  $t \neq t_k, k \in Z_+$ , differentiating  $V(t)$  along the solution of (4) gives:

$$\begin{aligned} D^+ V(t) &= 2 \sum_{i=1}^N e_i^T(t) P \dot{e}_i(t) \\ &= 2 \sum_{i=1}^N e_i^T(t) P \left[ -(\mathfrak{D} + \Delta \mathfrak{D}(t)) e_i(t) + (\mathfrak{E} + \Delta \mathfrak{E}(t)) \bar{\beta}(e_i(t)) \right. \\ &\quad \left. + (\mathfrak{F} + \Delta \mathfrak{F}(t)) \bar{\gamma}(e_i(t - \tau_1(t))) + \epsilon \sum_{j=1}^N b_{ij} \bar{\psi}(e_j(t - \tau_2(t))) \right]. \end{aligned} \tag{10}$$

Combining Assumption 2 and Lemma 1, one can obtain:

$$\begin{aligned} &2 \sum_{i=1}^N e_i^T(t) P [-(\mathfrak{D} + \Delta \mathfrak{D}(t))] e_i(t) \\ &= -2 \sum_{i=1}^N e_i^T(t) P (\mathfrak{D} + G_{\mathfrak{D}} \Omega(t) H_{\mathfrak{D}}) e_i(t) \\ &\leq -2 \sum_{i=1}^N e_i^T(t) P \mathfrak{D} e_i(t) + \sum_{i=1}^N \left[ \zeta_{\mathfrak{D}} e_i^T(t) P G_{\mathfrak{D}} G_{\mathfrak{D}}^T P e_i(t) + \zeta_{\mathfrak{D}}^{-1} e_i^T(t) \lambda_{\max}(H_{\mathfrak{D}}^T H_{\mathfrak{D}}) e_i(t) \right]. \end{aligned} \tag{11}$$

By Assumptions 1–2 and Lemma 1, one can derive:

$$\begin{aligned} &2 \sum_{i=1}^N e_i^T(t) P (\mathfrak{E} + \Delta \mathfrak{E}(t)) \bar{\beta}(e_i(t)) \\ &= 2 \sum_{i=1}^N e_i^T(t) P \mathfrak{E} \bar{\beta}(e_i(t)) + 2 \sum_{i=1}^N e_i^T(t) P G_{\mathfrak{E}} \Omega(t) H_{\mathfrak{E}} \bar{\beta}(e_i(t)) \\ &\leq \sum_{i=1}^N \left[ \zeta_{\mathfrak{E}} e_i^T(t) P \mathfrak{E} \mathfrak{E}^T P e_i(t) + \zeta_{\mathfrak{E}}^{-1} \bar{\beta}^T(e_i(t)) \bar{\beta}(e_i(t)) \right] \\ &\quad + \sum_{i=1}^N \left[ \zeta_{\mathfrak{E}} e_i^T(t) P G_{\mathfrak{E}} G_{\mathfrak{E}}^T P e_i(t) + \zeta_{\mathfrak{E}}^{-1} \bar{\beta}^T(e_i(t)) H_{\mathfrak{E}}^T H_{\mathfrak{E}} \bar{\beta}(e_i(t)) \right] \\ &\leq \sum_{i=1}^N \left[ \zeta_{\mathfrak{E}} e_i^T(t) P \mathfrak{E} \mathfrak{E}^T P e_i(t) + \zeta_{\mathfrak{E}} e_i^T(t) P G_{\mathfrak{E}} G_{\mathfrak{E}}^T P e_i(t) \right] \\ &\quad + \sum_{i=1}^N \left[ \zeta_{\mathfrak{E}}^{-1} + \zeta_{\mathfrak{E}}^{-1} \lambda_{\max}(H_{\mathfrak{E}}^T H_{\mathfrak{E}}) \right] L_{\bar{\beta}}^2 e_i^T(t) e_i(t). \end{aligned} \tag{12}$$

Similarly, one can further derive:

$$\begin{aligned}
 & 2 \sum_{i=1}^N e_i^T(t) P(\mathfrak{F} + \Delta \mathfrak{F}(t)) \bar{\gamma}(e_i(t - \tau_1(t))) \\
 = & 2 \sum_{i=1}^N e_i^T(t) P \mathfrak{F} \bar{\gamma}(e_i(t - \tau_1(t))) + 2 \sum_{i=1}^N e_i^T(t) P G_{\mathfrak{F}} \Omega(t) H_{\mathfrak{F}} \bar{\gamma}(e_i(t - \tau_1(t))) \\
 \leq & \sum_{i=1}^N \left[ \zeta_{\mathfrak{F}} e_i^T(t) P \mathfrak{F} \mathfrak{F}^T P e_i(t) + \zeta_{\mathfrak{F}}^{-1} \bar{\gamma}^T(e_i(t - \tau_1(t))) \bar{\gamma}(e_i(t - \tau_1(t))) \right] \\
 & + \sum_{i=1}^N \left[ \zeta_{\mathfrak{F}} e_i^T(t) P G_{\mathfrak{F}} G_{\mathfrak{F}}^T P e_i(t) + \zeta_{\mathfrak{F}}^{-1} \bar{\gamma}^T(e_i(t - \tau_1(t))) H_{\mathfrak{F}}^T H_{\mathfrak{F}} \bar{\gamma}(e_i(t - \tau_1(t))) \right] \\
 \leq & \sum_{i=1}^N \left[ \zeta_{\mathfrak{F}} e_i^T(t) P \mathfrak{F} \mathfrak{F}^T P e_i(t) + \zeta_{\mathfrak{F}} e_i^T(t) P G_{\mathfrak{F}} G_{\mathfrak{F}}^T P e_i(t) \right] \\
 & + \sum_{i=1}^N \left[ \zeta_{\mathfrak{F}}^{-1} + \zeta_{\mathfrak{F}}^{-1} \lambda_{\max}(H_{\mathfrak{F}}^T H_{\mathfrak{F}}) \right] L_{\gamma}^2 e_i^T(t - \tau_1(t)) e_i(t - \tau_1(t)). \tag{13}
 \end{aligned}$$

Based on Assumptions 1 and 3 and Lemma 1, one can obtain:

$$\begin{aligned}
 & 2 \sum_{i=1}^N e_i^T(t) P \epsilon \sum_{j=1}^N b_{ij} \bar{\psi}(e_j(t - \tau_2(t))) \\
 = & 2 \epsilon \sum_{i=1}^N \sum_{j=1}^N e_i^T(t) P b_{ij} \bar{\psi}(e_j(t - \tau_2(t))) \\
 \leq & \epsilon \sum_{i=1}^N \sum_{j=1}^N \delta e_i^T(t) P (b_{ij})^2 P e_i(t) + \epsilon \sum_{i=1}^N \sum_{j=1}^N \delta^{-1} \bar{\psi}^T(e_j(t - \tau_2(t))) \bar{\psi}(e_j(t - \tau_2(t))) \\
 \leq & \epsilon \sum_{i=1}^N \sum_{j=1}^N \delta e_i^T(t) P (b_{ij})^2 P e_i(t) + \epsilon \sum_{i=1}^N \sum_{j=1}^N \delta^{-1} L_{\psi}^2 e_j^T(t - \tau_2(t)) e_j(t - \tau_2(t)) \\
 \leq & \epsilon \delta M_b \sum_{i=1}^N e_i^T(t) P P e_i(t) + \epsilon \delta^{-1} L_{\psi}^2 N \sum_{i=1}^N e_i^T(t - \tau_2(t)) e_i(t - \tau_2(t)). \tag{14}
 \end{aligned}$$

Substituting inequalities (11)–(14) into (10), we have:

$$\begin{aligned}
 D^+ V(t) \leq & \sum_{i=1}^N e_i^T(t) \left[ -2P\mathfrak{D} + \zeta_{\mathfrak{D}} P G_{\mathfrak{D}} G_{\mathfrak{D}}^T P + \zeta_{\mathfrak{E}} P \mathfrak{E} \mathfrak{E}^T P + \zeta_{\mathfrak{F}} P \mathfrak{F} \mathfrak{F}^T P + \zeta_{\mathfrak{E}} P G_{\mathfrak{E}} G_{\mathfrak{E}}^T P \right. \\
 & + \zeta_{\mathfrak{F}} P G_{\mathfrak{F}} G_{\mathfrak{F}}^T P + \epsilon \delta M_b P P + \zeta_{\mathfrak{D}}^{-1} \lambda_{\max}(H_{\mathfrak{D}}^T H_{\mathfrak{D}}) I + (\zeta_{\mathfrak{E}}^{-1} + \zeta_{\mathfrak{E}}^{-1} \lambda_{\max}(H_{\mathfrak{E}}^T H_{\mathfrak{E}})) L_{\beta}^2 I \Big] e_i(t) \\
 & + \sum_{i=1}^N e_i^T(t - \tau_1(t)) \left[ \zeta_{\mathfrak{F}}^{-1} + \zeta_{\mathfrak{F}}^{-1} \lambda_{\max}(H_{\mathfrak{F}}^T H_{\mathfrak{F}}) \right] L_{\gamma}^2 e_i(t - \tau_1(t)) \\
 & + \sum_{i=1}^N e_i^T(t - \tau_2(t)) \left( \epsilon \delta^{-1} L_{\psi}^2 N \right) e_i(t - \tau_2(t)) \\
 \leq & \check{b}_0 V(t) + \check{b}_1 V(t - \tau_1(t)) + \check{b}_2 V(t - \tau_2(t)). \tag{15}
 \end{aligned}$$

When  $t = t_k, k \in Z_+$ , using the Lyapunov function definition and control protocol (3), one can derive that:

$$\begin{aligned}
 V(t_k) &= \sum_{i=1}^N e_i^T(t_k) P e_i(t_k) \\
 &= \sum_{i=1}^N \left[ (a_{ik} + 1) e_i^T(t_k^-) + c_{ik} e_i^T(t_k^- - \eta_k) \right] P \left[ (a_{ik} + 1) e_i(t_k^-) + c_{ik} e_i(t_k^- - \eta_k) \right] \\
 &\leq \bar{p} \sum_{i=1}^N \left[ (a_{ik} + 1)^2 e_i^T(t_k^-) e_i(t_k^-) + (a_{ik} + 1) c_{ik} e_i^T(t_k^-) e_i(t_k^- - \eta_k) \right. \\
 &\quad \left. + (a_{ik} + 1) c_{ik} e_i^T(t_k^- - \eta_k) e_i(t_k^-) + c_{ik}^2 e_i^T(t_k^- - \eta_k) e_i(t_k^- - \eta_k) \right] \\
 &\leq \bar{p} \sum_{i=1}^N \left[ 2(a_{ik} + 1)^2 e_i^T(t_k^-) e_i(t_k^-) + 2c_{ik}^2 e_i^T(t_k^- - \eta_k) e_i(t_k^- - \eta_k) \right] \\
 &\leq \bar{p} \sum_{i=1}^N \left[ a_k e_i^T(t_k^-) e_i(t_k^-) + c_k e_i^T(t_k^- - \eta_k) e_i(t_k^- - \eta_k) \right] \\
 &\leq \frac{\bar{p}}{p} \sum_{i=1}^N \left[ a_k e_i^T(t_k^-) P e_i(t_k^-) + c_k e_i^T(t_k^- - \eta_k) P e_i(t_k^- - \eta_k) \right] \\
 &\leq \frac{\bar{p}}{p} \left[ a_k V(t_k^-) + c_k V(t_k^- - \eta_k) \right]. \tag{16}
 \end{aligned}$$

Denote  $e(t) = [e_1^T(t), e_2^T(t), \dots, e_N^T(t)]^T$ . In view of Lemma 2, it follows from inequalities (15) and (16) that

$$V(t) \leq \frac{\sigma \mu(0) \bar{V}(0)}{\mu(t)}, \quad t \geq 0, \tag{17}$$

which further proclaims that

$$\|e(t)\| \leq \sqrt{\frac{\sigma \mu(0) \bar{p} |e(0)|^2}{p \mu(t)}}. \tag{18}$$

Hence, master–slave complex networks (1) and (2) can achieve  $\mu$ –synchronization via our control strategy, and we finish the mathematical derivation of Theorem 1.  $\square$

**Remark 6.** In [18–24], various interesting research results were derived based on the assumption that time delays are bound, that is  $0 \leq \tau_i(t) \leq \tau_i$ , where  $\tau_i$  represents a constant. Different from these existing works, we have removed the restrictive assumption on the upper bound of time delays, that is,  $0 \leq \tau_i(t) \leq \infty$ .

**Remark 7.** Considering that the  $\mu$ –synchronization between master–slave networks can convert to the  $\mu$ –stability of the corresponding error systems, the  $\mu$ –stability and  $\mu$ –synchronization have been investigated in [33–36], and the impacts of impulsive control strengths on system synchronization have been discussed in these works. Unlike these existing results, the influences of norm-bounded disturbances and non-delayed and delayed impulsive factors on synchronization, especially the influences of the impulse sampling delays of unidentified bounds, have been considered in this study.

When the concrete forms of time delays and  $\mu$ –function are determined, one can further obtain the following important corollaries, which indicate the close interconnection between  $\mu$ –synchronization and other mainstream synchronization modes.

**Corollary 1.** Suppose  $\mu(t) = (1 + p_1 t)^{p_2}$ ,  $\tau_1(t) = \omega_1 t$ ,  $\tau_2(t) = \omega_2 t$ , and  $\eta_k = \omega_3 t_k$ ,  $k \in Z_+$ , where  $p_1 > 0, p_2 > 0$ , and  $0 \leq \omega_i < 1 (i = 1, 2, 3)$ . When Assumptions 1–3 and conditions (ii)–(iv) are satisfied, if one can find suitable constants  $\sigma > 1, \xi > 0$ , and a matrix  $P = \text{diag}\{\bar{p}_1, \bar{p}_2, \dots, \bar{p}_n\} > 0$ , such that

$$|\check{b}_0| \xi + \sigma \left[ \frac{\check{b}_1}{(1 - \omega_1)^{p_2}} + \frac{\check{b}_2}{(1 - \omega_2)^{p_2}} \right] \xi < \ln \left[ \frac{\sigma}{(1 + p_1 \xi)^{p_2}} \right]$$

and

$$\left[ a_k \frac{\bar{p}}{p} + \frac{c_k}{(1 - \omega_3)^{p_2}} \frac{\bar{p}}{p} \right] \sigma \leq 1, k \in Z_+,$$

where  $a_k = \max\{2(a_{ik} + 1)^2, i = 1, 2, \dots, N\}$ ,  $c_k = \max\{2c_{ik}^2, i = 1, 2, \dots, N\}$ ,  $\bar{p} = \max\{\bar{p}_i, i = 1, 2, \dots, n\}$ , and  $p = \min\{\bar{p}_i, i = 1, 2, \dots, n\}$ , and then the power synchronization between master–slave dynamical networks (1) and (2) can be fulfilled through the hybrid delayed impulsive control.

**Proof.** Obviously, we just need to verify that the given function  $\mu(t) = (1 + p_1 t)^{p_2}$  satisfies Assumption 4. For any  $t \geq 0, k \in Z_+$ , we have:

$$\begin{aligned} \frac{\mu(t_k)}{\mu(t_{k-1})} &= \left[ \frac{1 + p_1 t_k}{1 + p_1 t_{k-1}} \right]^{p_2} = \left[ \frac{1 + p_1 t_{k-1} + p_1 (t_k - t_{k-1})}{1 + p_1 t_{k-1}} \right]^{p_2} \leq (1 + p_1 \xi)^{p_2}, \\ \frac{\mu(t)}{\mu^*(t - \tau_1(t))} &= \left[ \frac{1 + p_1 t}{1 + p_1 (1 - \omega_1) t} \right]^{p_2} = \frac{1}{\left[ \frac{1 + p_1 (1 - \omega_1) t}{1 + p_1 t} \right]^{p_2}} \leq \frac{1}{(1 - \omega_1)^{p_2}}, \\ \frac{\mu(t)}{\mu^*(t - \tau_2(t))} &= \left[ \frac{1 + p_1 t}{1 + p_1 (1 - \omega_2) t} \right]^{p_2} = \frac{1}{\left[ \frac{1 + p_1 (1 - \omega_2) t}{1 + p_1 t} \right]^{p_2}} \leq \frac{1}{(1 - \omega_2)^{p_2}}, \\ \frac{\mu(t_k)}{\mu^*(t_k - \eta_k)} &= \left[ \frac{1 + p_1 t_k}{1 + p_1 (1 - \omega_3) t_k} \right]^{p_2} = \frac{1}{\left[ \frac{1 + p_1 (1 - \omega_3) t_k}{1 + p_1 t_k} \right]^{p_2}} \leq \frac{1}{(1 - \omega_3)^{p_2}}. \end{aligned}$$

Based on the above inequalities and Assumption 4, let  $\mu_0 = (1 + p_1 \xi)^{p_2}$ ,  $\mu_1 = \frac{1}{(1 - \omega_1)^{p_2}}$ ,  $\mu_2 = \frac{1}{(1 - \omega_2)^{p_2}}$ , and  $\mu_3 = \frac{1}{(1 - \omega_3)^{p_2}}$ . Using the similar mathematical derivation of Theorem 1, one can obtain the power synchronization between master dynamical network (1) and slave dynamical network (2). □

**Corollary 2.** Assume  $\mu(t) = \ln(e + q_1 t)$ ,  $\tau_1(t) = t + [e - (t + e)^{\zeta_1}] / q_1$ ,  $\tau_2(t) = t + [e - (t + e)^{\zeta_2}] / q_1$ , and  $\eta_k = \omega_4 t_k$ ,  $k \in Z_+$ , where  $0 < q_1 < 1, 0 < \zeta_i < 1, (i = 1, 2)$ , and  $0 \leq \omega_4 < 1$ . When Assumptions 1–3 and conditions (ii)–(iv) are satisfied, if one can find appropriate constants  $\sigma > 1, \xi > 0$ , and a matrix  $P = \text{diag}\{\bar{p}_1, \bar{p}_2, \dots, \bar{p}_n\} > 0$ , such that

$$[|\check{b}_0| + \sigma \left( \frac{\check{b}_1}{\zeta_1} + \frac{\check{b}_2}{\zeta_2} \right)] \xi < \ln \left[ \frac{\sigma}{1 + \ln(1 + q_1 \xi / e)} \right],$$

and

$$\left[ a_k \frac{\bar{p}}{p} + c_k (1 - \ln(1 - \omega_4)) \frac{\bar{p}}{p} \right] \sigma \leq 1, k \in Z_+,$$

where  $a_k = \max\{2(a_{ik} + 1)^2, i = 1, 2, \dots, N\}$ ,  $c_k = \max\{2c_{ik}^2, i = 1, 2, \dots, N\}$ ,  $\bar{p} = \max\{\bar{p}_i, i = 1, 2, \dots, n\}$ , and  $p = \min\{\bar{p}_i, i = 1, 2, \dots, n\}$ , then the log synchronization between master–slave dynamical networks (1) and (2) can be fulfilled through the hybrid delayed impulsive control.

**Proof.** Evidently, we just need to validate Assumption 4. One can obtain

$$\begin{aligned} \frac{\mu(t_k)}{\mu(t_{k-1})} &= \frac{\ln(e + q_1 t_k)}{\ln(e + q_1 t_{k-1})} \leq 1 + \frac{\ln[1 + \frac{q_1(t_k - t_{k-1})}{e + q_1 t_{k-1}}]}{\ln(e + q_1 t_{k-1})} \leq 1 + \ln(1 + q_1 \zeta / e), \\ \frac{\mu(t)}{\mu^*(t - \tau_1(t))} &= \frac{\ln(e + q_1 t)}{\mu^*[(t + e)^{\zeta_1} - e] / q_1} = \frac{\ln(e + q_1 t)}{\zeta_1 \ln(e + t)} \leq \frac{1}{\zeta_1}, \\ \frac{\mu(t)}{\mu^*(t - \tau_2(t))} &= \frac{\ln(e + q_1 t)}{\mu^*[(t + e)^{\zeta_2} - e] / q_1} = \frac{\ln(e + q_1 t)}{\zeta_2 \ln(e + t)} \leq \frac{1}{\zeta_2}, \\ \frac{\mu(t_k)}{\mu^*(t_k - \eta_k)} &= \frac{\ln(e + q_1 t_k)}{\ln(e + q_1(t_k - \omega_4 t_k))} = 1 + \frac{\ln[\frac{e + q_1 t_k}{e + q_1(1 - \omega_4)t_k}]}{\ln[e + q_1(1 - \omega_4)t_k]} \leq 1 - \ln(1 - \omega_4), \end{aligned}$$

for any  $t \geq 0, k \in Z_+$ . Based on the above inequalities and Assumption 4, let  $\mu_0 = 1 + \ln(1 + q_1 \zeta / e)$ ,  $\mu_1 = \frac{1}{\zeta_1}$ ,  $\mu_2 = \frac{1}{\zeta_2}$ , and  $\mu_3 = 1 - \ln(1 - \omega_4)$ . Applying the analogous mathematical derivation of Theorem 1, we can obtain the log synchronization between master dynamical network (1) and slave dynamical network (2). □

**Corollary 3.** Assume  $\mu(t) = \exp(\omega t)$ ,  $0 \leq \tau_i(t) \leq \tau (i = 1, 2)$ ,  $0 \leq \eta_k \leq \eta, k \in Z_+$ , where  $\omega > 0$ . When Assumptions 1–3 and conditions (ii)–(iv) are satisfied, if one can find appropriate constants  $\sigma > 1, \zeta > 0$ , and a matrix  $P = \text{diag}\{\bar{p}_1, \bar{p}_2, \dots, \bar{p}_n\} > 0$ , such that

$$[|\check{b}_0| + \sigma(\check{b}_1 + \check{b}_2)\exp(\omega\tau)]\zeta < \ln\left[\frac{\sigma}{\exp(\omega\zeta)}\right],$$

and

$$[a_k \frac{\bar{p}}{p} + c_k \exp(\omega\eta) \frac{\bar{p}}{p}]\sigma \leq 1, k \in Z_+,$$

where  $a_k = \max\{2(a_{ik} + 1)^2, i = 1, 2, \dots, N\}$ ,  $c_k = \max\{2c_{ik}^2, i = 1, 2, \dots, N\}$ ,  $\bar{p} = \max\{\bar{p}_i, i = 1, 2, \dots, n\}$ , and  $p = \min\{\bar{p}_i, i = 1, 2, \dots, n\}$ , then the exponential synchronization between master–slave dynamical networks (1) and (2) can be fulfilled through the hybrid delayed impulsive control.

**Proof.** Evidently, we only need to explain that Assumption 4 holds for  $\mu(t) = \exp(\omega t)$ . One can obtain

$$\begin{aligned} \frac{\mu(t_k)}{\mu(t_{k-1})} &= \frac{\exp(\omega t_k)}{\exp(\omega t_{k-1})} = \exp[\omega(t_k - t_{k-1})] \leq \exp(\omega\zeta), \\ \frac{\mu(t)}{\mu^*(t - \tau_1(t))} &= \frac{\exp(\omega t)}{\exp[\omega(t - \tau_1(t))]} = \exp[\omega\tau_1(t)] \leq \exp(\omega\tau), \\ \frac{\mu(t)}{\mu^*(t - \tau_2(t))} &= \frac{\exp(\omega t)}{\exp[\omega(t - \tau_2(t))]} = \exp[\omega\tau_2(t)] \leq \exp(\omega\tau), \\ \frac{\mu(t_k)}{\mu^*(t_k - \eta_k)} &= \frac{\exp(\omega t_k)}{\exp[\omega(t_k - \eta_k)]} = \exp[\omega\eta_k] \leq \exp(\omega\eta), \end{aligned}$$

for any  $t \geq 0, k \in Z_+$ . Let  $\mu_0 = \exp(\omega\zeta)$ ,  $\mu_1 = \exp(\omega\tau)$ ,  $\mu_2 = \exp(\omega\tau)$ , and  $\mu_3 = \exp(\omega\eta)$ . Using a similar mathematical derivation, we can easily obtain Corollary 3. □

#### 4. Numerical Examples

We present three numerical simulations to explicate the correctness of the theoretical achievements derived above.

**Example 1.** Contemplate a two-dimensional complex dynamical network consisting of six nodes involving variable delays of unidentified bounds as below:

$$\begin{aligned} \dot{u}_i(t) = & -(\mathfrak{D} + \Delta\mathfrak{D}(t))u_i(t) + (\mathfrak{E} + \Delta\mathfrak{E}(t))\beta(u_i(t)) + (\mathfrak{F} + \Delta\mathfrak{F}(t))\gamma(u_i(t - \tau_1(t))) \\ & + \epsilon \sum_{j=1}^6 b_{ij}\psi(u_j(t - \tau_2(t))), \quad i = 1, 2, \dots, 6, \end{aligned} \tag{19}$$

where  $u_i(t) = (u_{1i}(t), u_{2i}(t))^T$  represents the two-dimensional state vector of node  $i$ . Choose the nonlinear mappings  $\beta(u_i(t)) = \gamma(u_i(t)) = 1/5(\tanh(u_{1i}(t)), \tanh(u_{2i}(t)))^T$  as activation functions, and select the mapping  $\psi(u_i(t)) = 1/4(\tanh(u_{1i}(t)), \tanh(u_{2i}(t)))^T$  as the coupling function. Taking dynamical network (19) as the master system, then the slave system under hybrid impulsive effects can be given by

$$\begin{cases} \dot{v}_i(t) = -(\mathfrak{D} + \Delta\mathfrak{D}(t))v_i(t) + (\mathfrak{E} + \Delta\mathfrak{E}(t))\beta(v_i(t)) + (\mathfrak{F} + \Delta\mathfrak{F}(t))\gamma(v_i(t - \tau_1(t))) \\ \quad + \epsilon \sum_{j=1}^6 b_{ij}\psi(v_j(t - \tau_2(t))), \quad t \neq t_k, \\ \Delta e_i(t_k) = a_{ik}e_i(t_k^-) + c_{ik}e_i(t_k^- - \eta_k), \quad t = t_k, \quad k \in \mathbb{Z}_+, \end{cases} \tag{20}$$

where  $v_i(t) = (v_{1i}(t), v_{2i}(t))^T$  represents the state vector of node  $i$ . The connection synaptic matrices  $\mathfrak{D}$ ,  $\mathfrak{E}$ , and  $\mathfrak{F}$  can be selected as:

$$\mathfrak{D} = \begin{bmatrix} 1 & 0 \\ 0 & 1 \end{bmatrix}, \mathfrak{E} = \begin{bmatrix} 2.0 & -0.1 \\ -3.0 & 1.5 \end{bmatrix}, \mathfrak{F} = \begin{bmatrix} -1.5 & -0.1 \\ -0.2 & -2.0 \end{bmatrix}.$$

The bounded time-varying disturbances can be chosen as:

$$\begin{aligned} \Delta\mathfrak{D}(t) &= G_{\mathfrak{D}}\Omega(t)H_{\mathfrak{D}} = \begin{bmatrix} 0.1 & 0 \\ 0 & 0.1 \end{bmatrix} \begin{bmatrix} \sin(t) & 0 \\ 0 & \cos(t) \end{bmatrix} \begin{bmatrix} 0.05 & 0 \\ 0 & 0.05 \end{bmatrix}, \\ \Delta\mathfrak{E}(t) &= G_{\mathfrak{E}}\Omega(t)H_{\mathfrak{E}} = \begin{bmatrix} 0.2 & 0 \\ 0 & 0.2 \end{bmatrix} \begin{bmatrix} \sin(t) & 0 \\ 0 & \cos(t) \end{bmatrix} \begin{bmatrix} 0.15 & 0 \\ 0 & 0.15 \end{bmatrix}, \\ \Delta\mathfrak{F}(t) &= G_{\mathfrak{F}}\Omega(t)H_{\mathfrak{F}} = \begin{bmatrix} 0.3 & 0 \\ 0 & 0.3 \end{bmatrix} \begin{bmatrix} \sin(t) & 0 \\ 0 & \cos(t) \end{bmatrix} \begin{bmatrix} 0.25 & 0 \\ 0 & 0.25 \end{bmatrix}. \end{aligned}$$

The outer coupling matrix  $B$  is not restricted by the zero-row-sum condition or dissipative coupling condition, which can be chosen as:

$$B = \begin{bmatrix} 0 & 0 & 0.5 & 0 & 0.5 & 0.5 \\ 0.5 & 0 & 0.5 & 0.5 & 0.5 & 0 \\ 0 & 0.5 & 0 & 0.5 & 0 & 0.5 \\ 0.5 & 0 & 0.5 & 0 & 0.5 & 0 \\ 0.5 & 0.5 & 0 & 0.5 & 0 & 0.5 \\ 0.5 & 0 & 0.5 & 0.5 & 0.5 & 0 \end{bmatrix}.$$

The master network and the slave network have the same node size. In the simulation, the six nodes in the master network and the slave network are connected one-to-one. Through a simple computation, one can easily derive  $L_{\beta} = L_{\gamma} = 1/5$  and  $L_{\psi} = 1/4$ , which satisfies Assumption 1. Clearly,  $\Omega^T(t)\Omega(t) \leq I$  shows that Assumption 2 holds. When  $M_b = 3$ , Assumption 3 can be fulfilled evidently. For convenience, three kinds of time-varying delays are set in linear form as  $\tau_1(t) = \tau_2(t) = 0.01t$ ,  $\eta_k = t_k/6, k \in \mathbb{Z}_+$ . It should be emphasized that their boundaries are unidentified and evolve towards infinity over time. Choose  $\zeta_{\mathfrak{D}} = \zeta_{\mathfrak{E}} = 2, \zeta_{\mathfrak{F}} = 4, \zeta_{\mathfrak{E}} = \zeta_{\mathfrak{F}} = 0.1, \sigma = 2.43, \delta = 0.5, \epsilon = 0.05, \bar{p} = \underline{p} = 1.62, \mu(t) = \sqrt{1 + 3t}$ . The impulsive sequences  $\{t_k\}$  satisfy  $t_k - t_{k-1} \leq 0.01$

for any  $k \in Z_+$ . Calculation results yield  $\mu_0 = 1.0149$ ,  $\mu_1 = 1.0050$ ,  $\mu_2 = 1.0050$ , and  $\mu_3 = 1.0954$ . Impulsive strengths are key parameters that decide whether the master and slave systems can be synchronized. When parameters  $p_i, \mu_i, \sigma$  are determined, one can select suitable impulsive strengths according to the second condition in Corollary 1. In this simulation, we can set  $a_{ik} = -0.7, c_{ik} = 0.3$ . Moreover, when  $\check{b}_0 = 73.5, \check{b}_1 = 1.01, \check{b}_2 = 1.12$ , one can obtain  $|\check{b}_0|\check{\xi} + \sigma \left[ \frac{\check{b}_1}{(1-\omega_1)^{p_2}} + \frac{\check{b}_2}{(1-\omega_2)^{p_2}} \right] \check{\xi} - \ln \left[ \frac{\sigma}{(1+p_1\check{\xi})^{p_2}} \right] = -0.0861 < 0$ , and  $[a_k \frac{\check{p}}{p} + \frac{c_k}{(1-\omega_3)^{p_2}} \frac{\check{p}}{p}] \sigma - 1 = -0.0835 < 0$ . Hence, it is not difficult to find that all the constraint circumstances in Corollary 1 are valid.

The initial conditions of complex dynamical networks are generated randomly in  $[-30, 30]$ . The four-step Runge–Kutta approach gives the numerical simulation results of Corollary 1 with impulsive strengths  $a_{ik} = -0.7$  and  $c_{ik} = 0.3$ , as seen in Figure 2. The horizontal axis represents the evolution time  $t$ , which is measured in seconds. The ordinate is the norm of the error vector. It is dimensionless and characterizes the magnitude of the error. Figure 2 displays the state trajectories of different error norm curves with time evolution. As we can see in the six subgraphs, the error of each node in the master and slave systems gradually approaches 0. According to the definition of synchronization, we can obtain that the objective of power synchronization between slave network (20) and master network (19) can be accomplished under hybrid impulsive control schemes. Furthermore, to investigate the influence of impulses on synchronization, the non-delayed impulse remains unchanged, and only the delayed impulsive strength is slightly adjusted to  $c_{ik} = 0.4$ , which makes  $[a_k \frac{\check{p}}{p} + \frac{c_k}{(1-\omega_3)^{p_2}} \frac{\check{p}}{p}] \sigma - 1 = 0.2892 > 0$  and the second condition of Corollary 1 not hold. Under this control strength, Figure 3 shows the state trajectories of six error norm curves with time evolution. From the six different subgraphs, it can be seen that the error between each node of the two systems slowly decreases, but it can never approach 0. According to the definition of synchronization, Figure 3 indicates that the power synchronization between networks (20) and (19) cannot be accomplished. This is mainly because the strength of the control cannot meet the given requirements.

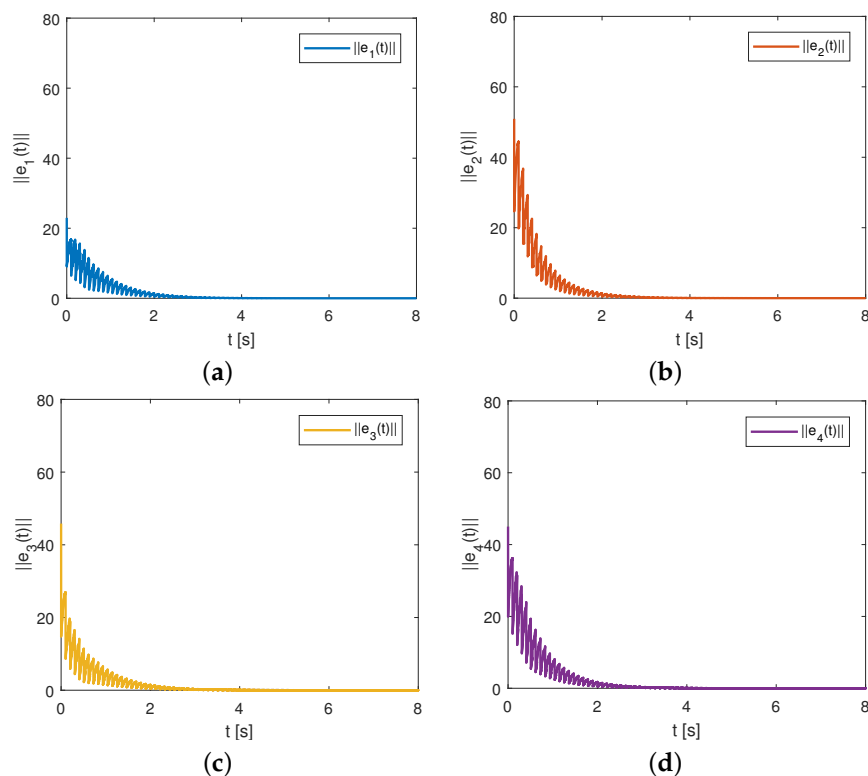
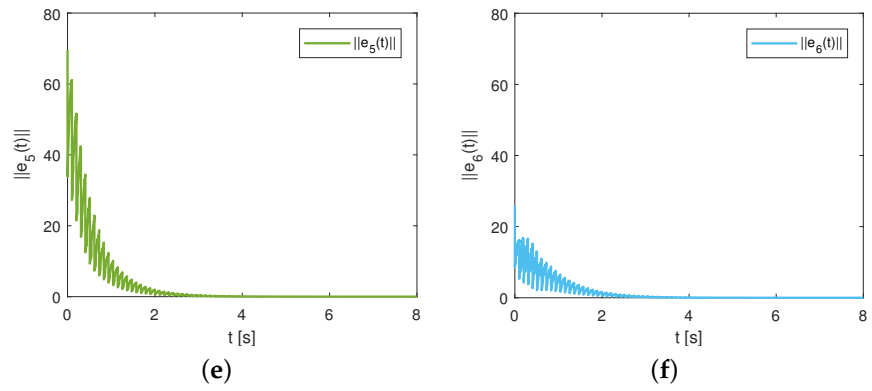
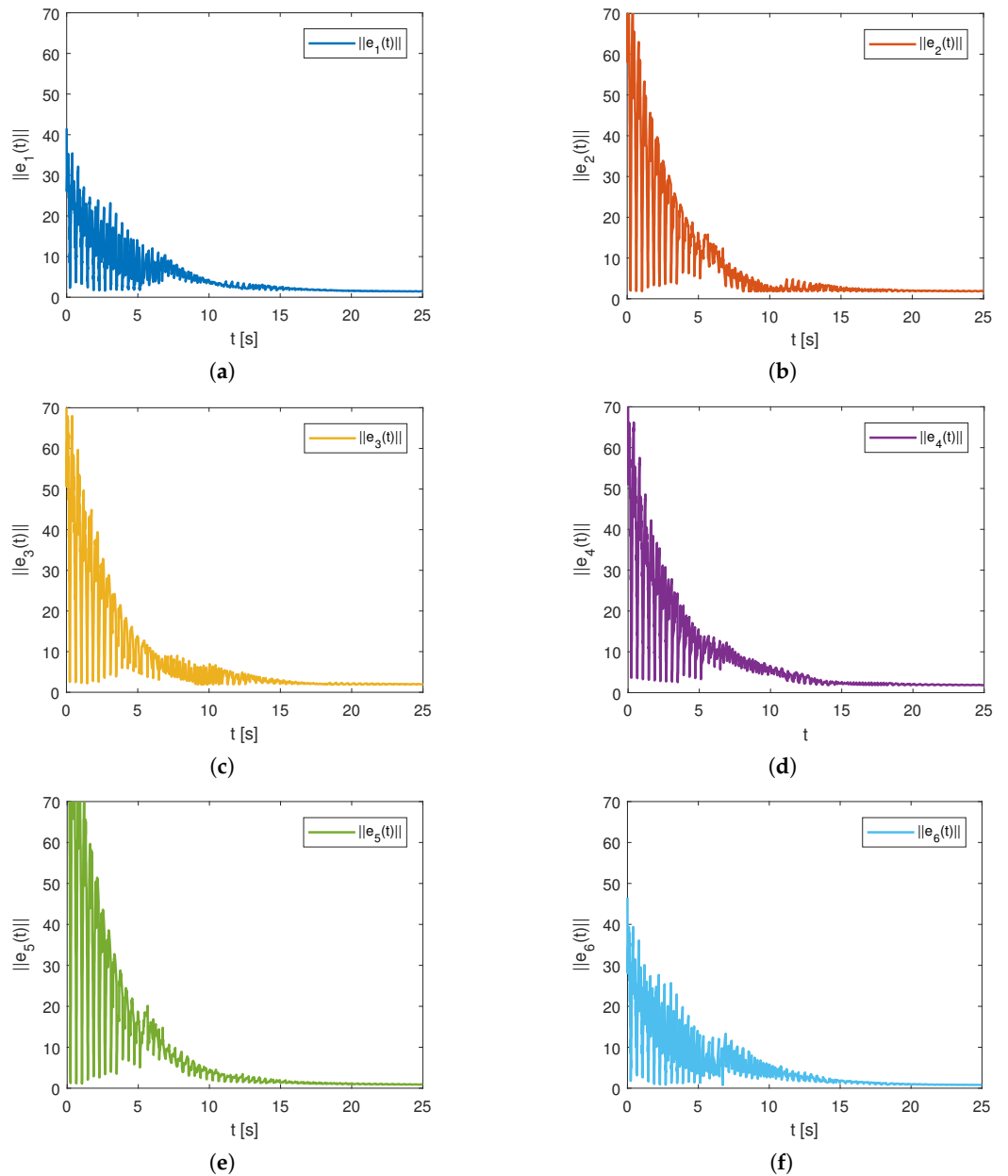


Figure 2. Cont.



**Figure 2.** The state trajectories of  $\|e_i(t)\|$  under impulsive control strengths  $a_{ik} = -0.7$  and  $c_{ik} = 0.3$  in Example 1. (a)  $\|e_1(t)\|$ ; (b)  $\|e_2(t)\|$ ; (c)  $\|e_3(t)\|$ ; (d)  $\|e_4(t)\|$ ; (e)  $\|e_5(t)\|$ ; (f)  $\|e_6(t)\|$ .



**Figure 3.** The state trajectories of  $\|e_i(t)\|$  under impulsive control strengths  $a_{ik} = -0.7$  and  $c_{ik} = 0.4$  in Example 1. (a)  $\|e_1(t)\|$ ; (b)  $\|e_2(t)\|$ ; (c)  $\|e_3(t)\|$ ; (d)  $\|e_4(t)\|$ ; (e)  $\|e_5(t)\|$ ; (f)  $\|e_6(t)\|$ .

**Remark 8.** In contrast to the impulsive control schemes in [15–17], the impulsive controller in this paper includes both the non-delayed effect and the delayed effect, in which both current and historical information are considered. It can effectively downgrade control duration and costs.

**Example 2.** Consider the similar two-dimensional master dynamical network and slave dynamical network as in Example 1. Different from the previous example, we not only change the uncertain disturbances and network topology architecture but also replace linear forms of time delays with more complex nonlinear expressions. Select the time-varying disturbances with finite boundaries as follows:

$$\Delta\mathfrak{D}(t) = G_{\mathfrak{D}}\Omega(t)H_{\mathfrak{D}} = \begin{bmatrix} 0.08 & 0 \\ 0 & 0.08 \end{bmatrix} \begin{bmatrix} \sin(t) \cos(t) & 0 \\ 0 & \sin(t) \cos(t) \end{bmatrix} \begin{bmatrix} 0.06 & 0 \\ 0 & 0.06 \end{bmatrix},$$

$$\Delta\mathfrak{E}(t) = G_{\mathfrak{E}}\Omega(t)H_{\mathfrak{E}} = \begin{bmatrix} 0.14 & 0 \\ 0 & 0.14 \end{bmatrix} \begin{bmatrix} \sin(t) \cos(t) & 0 \\ 0 & \sin(t) \cos(t) \end{bmatrix} \begin{bmatrix} 0.12 & 0 \\ 0 & 0.12 \end{bmatrix},$$

$$\Delta\mathfrak{F}(t) = G_{\mathfrak{F}}\Omega(t)H_{\mathfrak{F}} = \begin{bmatrix} 0.18 & 0 \\ 0 & 0.18 \end{bmatrix} \begin{bmatrix} \sin(t) \cos(t) & 0 \\ 0 & \sin(t) \cos(t) \end{bmatrix} \begin{bmatrix} 0.16 & 0 \\ 0 & 0.16 \end{bmatrix}.$$

Without the condition limitation of dissipative coupling, the outer coupling matrix representing the network topology with different weights can be selected as:

$$B = \begin{bmatrix} 0 & 0.2 & 0.1 & 0 & 0.3 & 0.4 \\ 0.2 & 0 & 0.3 & 0.1 & 0.2 & 0 \\ 0.1 & 0.6 & 0 & 0.2 & 0 & 0.3 \\ 0.2 & 0 & 0.4 & 0 & 0.5 & 0.1 \\ 0.1 & 0.4 & 0 & 0.2 & 0 & 0.3 \\ 0.1 & 0 & 0.3 & 0.1 & 0.4 & 0 \end{bmatrix}.$$

For the internal delay and the coupling delay, complex nonlinear time delays are used instead of linear time delays; that is,  $\tau_1(t) = \tau_2(t) = t + 5[e - (t + e)^{0.5}]$ . Assumption 3 could be established when  $M_b = 1$  and  $\Omega^T(t)\Omega(t) \leq I$  for  $\Omega(t) = \text{diag}\{\sin(t) \cos(t), \sin(t) \cos(t)\}$ . Choose  $\mu(t) = \ln(e + t/5)$ ,  $\eta_k = t_k/5, k \in Z_+, \bar{p} = \underline{p} = 1.60$ , and the other system parameters are chosen as in Example 1. Simple calculation yields that  $\mu_0 = 1.0007$ ,  $\mu_1 = 2$ ,  $\mu_2 = 2$ , and  $\mu_3 = 1.2231$ . Additionally, when  $\check{b}_0 = 68.29$ ,  $\check{b}_1 = 1.03$ ,  $\check{b}_2 = 1.05$ , one can further obtain  $[|\check{b}_0| + \sigma(\frac{\check{b}_1}{\check{c}_1} + \frac{\check{b}_2}{\check{c}_2})]\check{\xi} - \ln\left[\frac{\sigma}{1 + \ln(1 + q_1\check{\xi}/e)}\right] = -0.1032 < 0$ , and  $\left[a_k \frac{\bar{p}}{\underline{p}} + c_k(1 - \ln(1 - \omega_4)) \frac{\bar{p}}{\underline{p}}\right]\sigma - 1 = -0.0276 < 0$ . Hence, one can find that all the constraint circumstances in Corollary 2 hold.

The initial conditions of complex dynamical networks are generated randomly as before, and one can see the simulation results of Corollary 2 in Figure 4. Under impulsive strengths  $a_{ik} = -0.7$  and  $c_{ik} = 0.3$ , Figure 4 displays the state trajectories of  $\|e_i(t)\|$  with time evolution, which shows that the objective of log synchronization between the master network and the corresponding slave network can also be achieved. In addition, to observe the influence of the non-delayed impulsive strength on log synchronization, keep the delayed impulsive strength unchanged and slightly adjust the other impulsive strength to  $a_{ik} = -0.6$ , which makes  $\left[a_k \frac{\bar{p}}{\underline{p}} + c_k(1 - \ln(1 - \omega_4)) \frac{\bar{p}}{\underline{p}}\right]\sigma - 1 = 0.3126 > 0$  and breaks the second condition of Corollary 2. Under this circumstance and impulsive strengths, Figure 5 indicates that the state trajectories of  $\|e_i(t)\|$  cannot approach zero as control time evolves, which suggests that log synchronization cannot be fulfilled between master-slave dynamical networks.

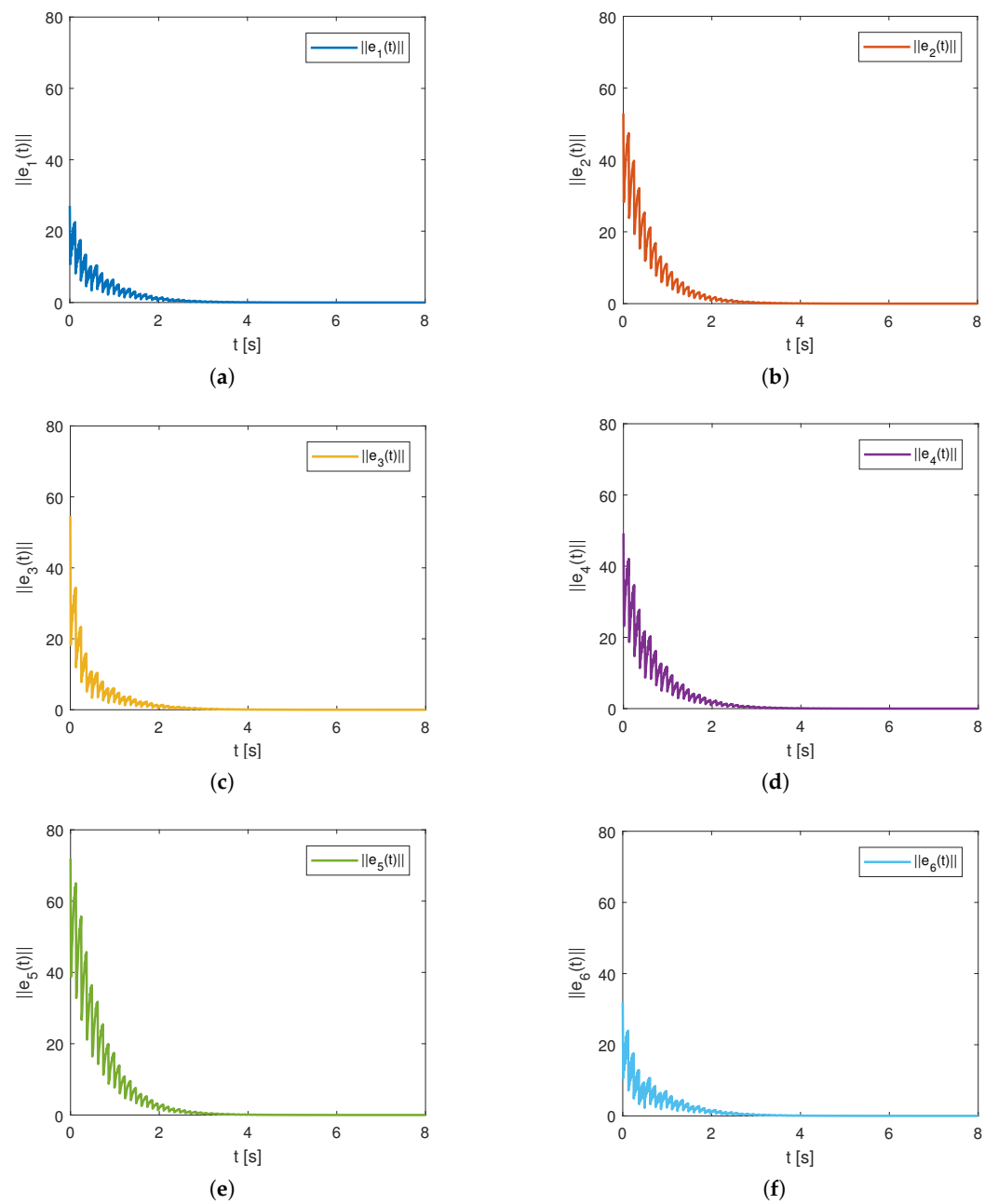


**Figure 4.** The state trajectories of  $\|e_i(t)\|$  under impulsive control strengths  $a_{ik} = -0.7$  and  $c_{ik} = 0.3$  in Example 2. (a)  $\|e_1(t)\|$ ; (b)  $\|e_2(t)\|$ ; (c)  $\|e_3(t)\|$ ; (d)  $\|e_4(t)\|$ ; (e)  $\|e_5(t)\|$ ; (f)  $\|e_6(t)\|$ .

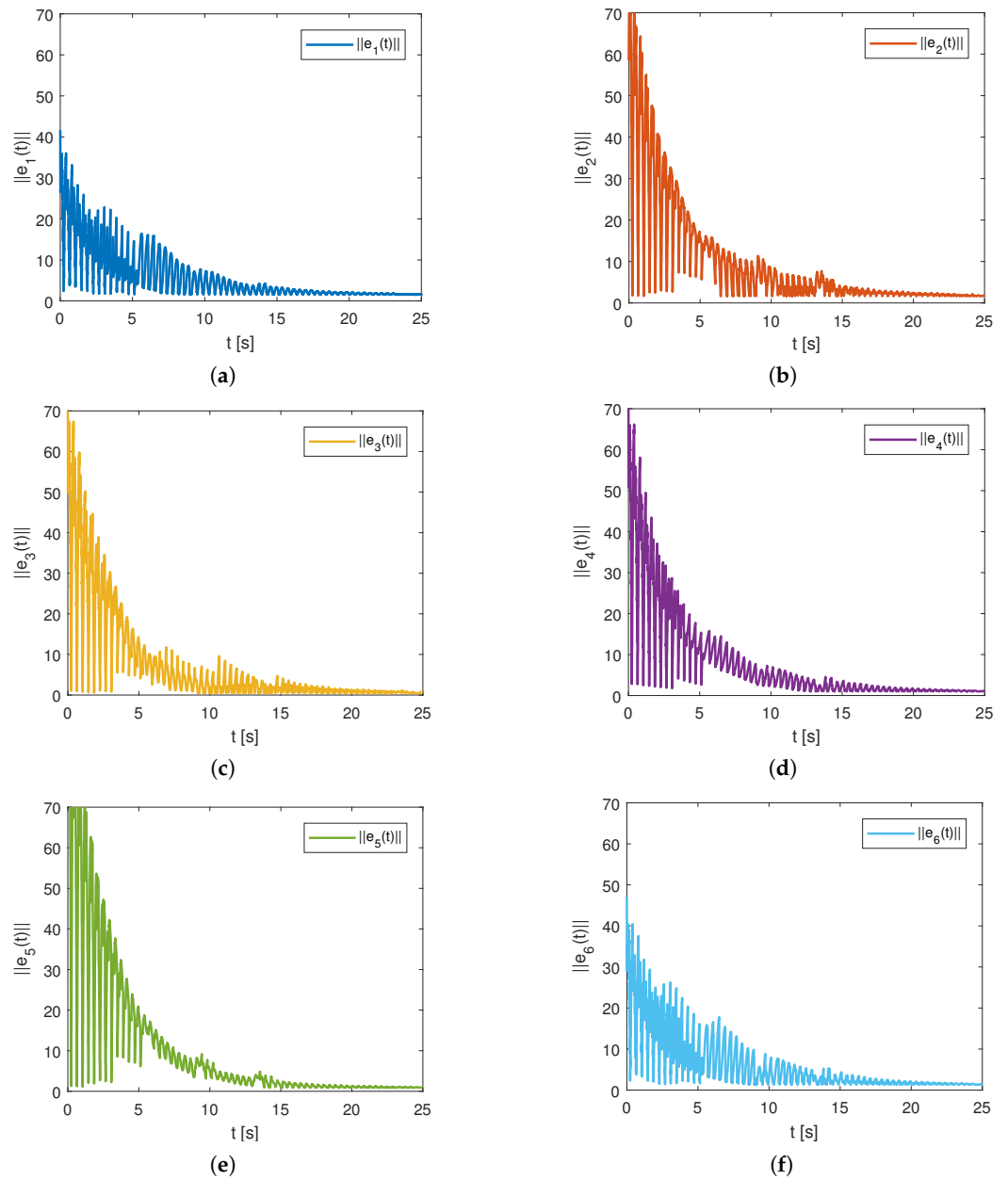


**Figure 5.** The state trajectories of  $\|e_i(t)\|$  under impulsive control strengths  $a_{ik} = -0.6$  and  $c_{ik} = 0.3$  in Example 2. (a)  $\|e_1(t)\|$ ; (b)  $\|e_2(t)\|$ ; (c)  $\|e_3(t)\|$ ; (d)  $\|e_4(t)\|$ ; (e)  $\|e_5(t)\|$ ; (f)  $\|e_6(t)\|$ .

**Example 3.** Consider a two-dimensional master network including six nodes, in which each uncoupled node can be described by a chaotic dynamical system. Unlike in previous examples, the first activation function is  $\beta(u_i(t)) = (\tanh(u_{1i}(t)), \tanh(u_{2i}(t)))^T$ , and the second activation function is  $\gamma(u_i(t)) = (0.5(|u_{1i}(t) + 1| - |u_{1i}(t) - 1|), 0.5(|u_{2i}(t) + 1| - |u_{2i}(t) - 1|))^T$ . The connection synaptic matrices  $\mathfrak{D}$ ,  $\mathfrak{E}$ , and  $\mathfrak{F}$  can be selected as:

$$\mathfrak{D} = \begin{bmatrix} 1 & 0 \\ 0 & 1 \end{bmatrix}, \mathfrak{E} = \begin{bmatrix} 1 + \frac{\pi}{4} & 20 \\ 0.1 & 1 + \frac{\pi}{4} \end{bmatrix}, \mathfrak{F} = \begin{bmatrix} -\frac{1.3\sqrt{2}\pi}{4} & 0.1 \\ 0.1 & -\frac{1.3\sqrt{2}\pi}{4} \end{bmatrix}.$$

The disturbances, including constant matrices and bounded time-varying matrices, are given by:

$$\Delta\mathfrak{D}(t) = G_{\mathfrak{D}}\Omega(t)H_{\mathfrak{D}} = \begin{bmatrix} 0.36 & 0 \\ 0 & 0.36 \end{bmatrix} \begin{bmatrix} \frac{|\sin(t)\cos(t)|}{2} & 0 \\ 0 & \frac{|\sin(t)\cos(t)|}{2} \end{bmatrix} \begin{bmatrix} 0.14 & 0 \\ 0 & 0.14 \end{bmatrix},$$

$$\Delta \mathbf{e}(t) = G_{\mathbf{e}} \Omega(t) H_{\mathbf{e}} = \begin{bmatrix} 0.08 & 0 \\ 0 & 0.08 \end{bmatrix} \begin{bmatrix} \frac{|\sin(t) \cos(t)|}{2} & 0 \\ 0 & \frac{|\sin(t) \cos(t)|}{2} \end{bmatrix} \begin{bmatrix} 0.10 & 0 \\ 0 & 0.10 \end{bmatrix},$$

$$\Delta \mathbf{f}(t) = G_{\mathbf{f}} \Omega(t) H_{\mathbf{f}} = \begin{bmatrix} 0.42 & 0 \\ 0 & 0.42 \end{bmatrix} \begin{bmatrix} \frac{|\sin(t) \cos(t)|}{2} & 0 \\ 0 & \frac{|\sin(t) \cos(t)|}{2} \end{bmatrix} \begin{bmatrix} 0.24 & 0 \\ 0 & 0.24 \end{bmatrix}.$$

Consider the nonlinear internal delay and coupling delay as  $\tau_1(t) = \frac{e^t}{1+e^t}, \tau_2(t) = \frac{0.1e^t}{1+e^t}$ , which are time-varying and satisfy  $0 < \tau_i(t) < 1$ . It is not difficult to validate that all assumptions are established when  $M_b = 1$ . Choose  $\mu(t) = \exp(0.1t), \eta_k = 0.1, k \in Z_+$ ,  $\bar{p} = p = 1.43$ . The coupled network structure is the same as in the previous example. Simple calculation gives  $\mu_0 = 1.001, \mu_1 = 1.1052, \mu_2 = 1.1052$ , and  $\mu_3 = 1.0101$ . Additionally, when  $\check{b}_0 = 62.34, \check{b}_1 = 1.04, \check{b}_2 = 1.06$ , one can further obtain  $[\check{b}_0 + \sigma(\check{b}_1 + \check{b}_2)\exp(\omega\tau)]\check{\zeta} - \ln\left[\frac{\sigma}{\exp(\omega\check{\zeta})}\right] = -0.0823 < 0$ , and  $[a_k \frac{\bar{p}}{p} + c_k \exp(\omega\eta) \frac{\bar{p}}{p}]\sigma - 1 = -0.2092 < 0$ . Hence, it is clear that all the constraint circumstances in Corollary 3 are satisfied.

The initial values of complex networks are still randomly generated. First, two impulsive strengths are set as  $a_{ik} = -0.65$  and  $c_{ik} = 0.25$ . Figure 6 gives the state error between master–slave networks with time evolution, which shows that exponential synchronization can be achieved in this case. Additionally, adjusting the control intensities as  $a_{ik} = -0.60$  and  $c_{ik} = 0.35$  makes  $[a_k \frac{\bar{p}}{p} + c_k \exp(\omega\eta) \frac{\bar{p}}{p}]\sigma - 1 = 0.2087 > 0$ , and some conditions of Corollary 3 cannot be guaranteed. In such control circumstances, Figure 7 gives the state trajectories of  $\|e_i(t)\|$  with time variation. Observation shows that the synchronization error of each neuron cannot approach zero under control and synchronization fails. The above experiments indicate that the impulsive intensities have an important influence on the stability of the error system. Minor changes in strengths may cause the synchronization target to not be completed.

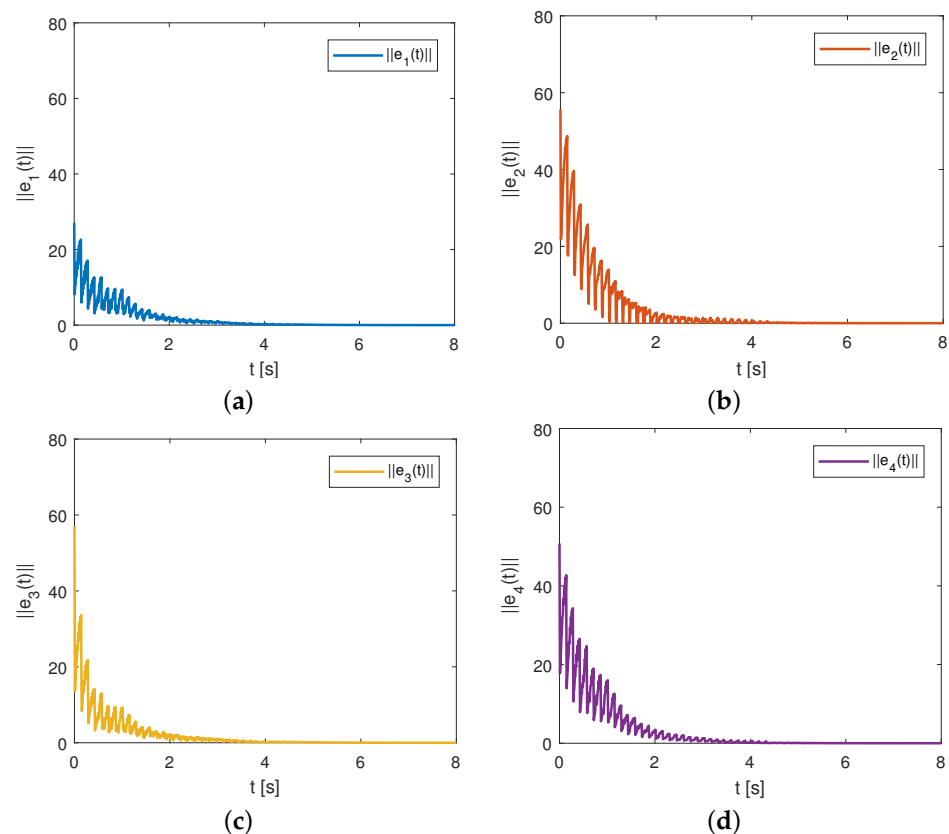
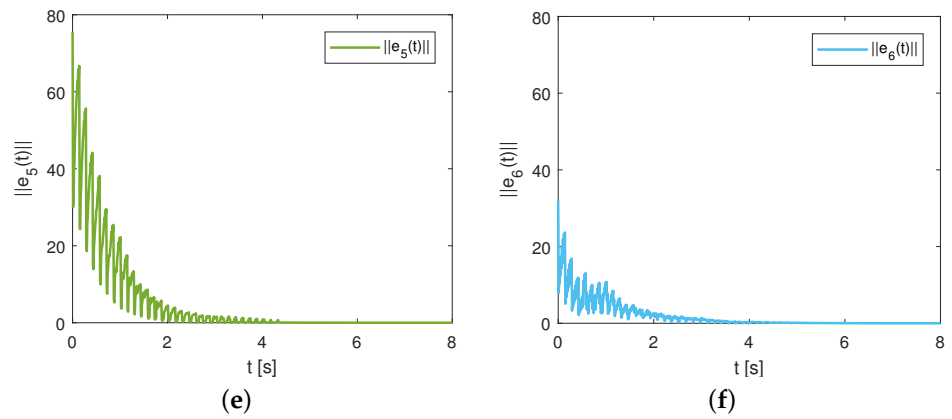
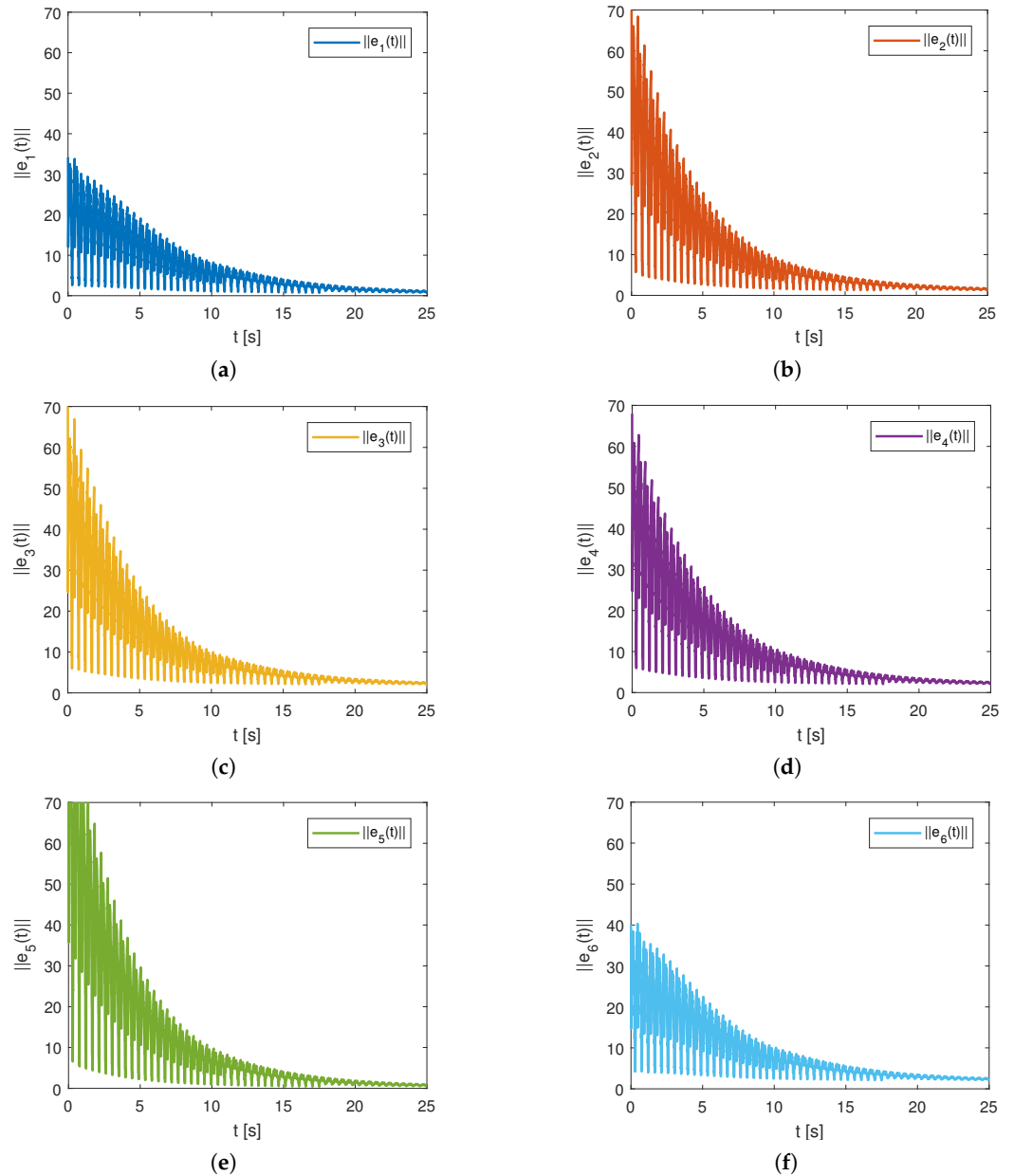


Figure 6. Cont.



**Figure 6.** The state trajectories of  $\|e_i(t)\|$  under impulsive control strengths  $a_{ik} = -0.65$  and  $c_{ik} = 0.25$  in Example 3. (a)  $\|e_1(t)\|$ ; (b)  $\|e_2(t)\|$ ; (c)  $\|e_3(t)\|$ ; (d)  $\|e_4(t)\|$ ; (e)  $\|e_5(t)\|$ ; (f)  $\|e_6(t)\|$ .



**Figure 7.** The state trajectories of  $\|e_i(t)\|$  under impulsive control strengths  $a_{ik} = -0.60$  and  $c_{ik} = 0.35$  in Example 3. (a)  $\|e_1(t)\|$ ; (b)  $\|e_2(t)\|$ ; (c)  $\|e_3(t)\|$ ; (d)  $\|e_4(t)\|$ ; (e)  $\|e_5(t)\|$ ; (f)  $\|e_6(t)\|$ .

**Remark 9.** Different from the results in [33–35], this article shows that  $\mu$ -synchronization of complex networks is equivalent to  $\mu$ -stability of the corresponding error system and reveals the inner link between  $\mu$ -synchronization and other synchronization patterns, such as power synchronization, log synchronization, exponential synchronization, etc.

## 5. Conclusions

This article explored the synchronization challenge for a type of non-dissipative coupled complex network comprising bounded disturbances and time-varying delays of unidentified bounds. Based on the hybrid non-delayed and delayed impulsive control techniques, the impact of three types of time delays with unidentified bounds on system stability can be effectively overcome by transforming  $\mu$ -synchronization issues into  $\mu$ -stability issues. Removing the zero-row-sum constraint of the topological matrix and the straitjacket of time delay on impulse intervals, some new synchronization criteria for the controlled model can be obtained and verified by numerical examples. Our future research direction is to set appropriate impulse event-triggered mechanisms to solve stability and synchronization problems in high-order complex dynamical networks with distributed time delays of unidentified bounds.

**Author Contributions:** Conceptualization, K.S., H.W. and H.F.; methodology, H.W., K.S. and H.F.; software, Y.X., R.Z. and S.Z.; writing—original draft, H.F., H.W. and K.S.; writing—review and editing, H.F., Y.X., R.Z. and S.Z. All authors have read and agreed to the published version of the manuscript.

**Funding:** This work was supported by the Open Foundation of Engineering Research Center of Big Data Application in Private Health Medicine, Fujian Province University, under Grant (MKF202201), the Sichuan Science and Technology Program under Grant (21YYJC0469), the Program of Science and Technology of Sichuan Province of China under Grant (2021ZYD0012), the Key R&D Projects of Sichuan Provincial Department of Science and Technology under Grant (2023YFG0287), the Introducing Talent Projects of Putian University Seedling Fund under Grant (2019110), and the Natural Science Foundation of Fujian Province under Grant (2022J011171, 2022J011170, 2023J011015).

**Data Availability Statement:** Not applicable.

**Conflicts of Interest:** The authors declare no conflicts of interest.

## References

1. Mani, P.; Rajan, R.; Shanmugam, L.; Joo, Y.H. Adaptive control for fractional order induced chaotic fuzzy cellular neural networks and its application to image encryption. *Inf. Sci.* **2019**, *491*, 74–89. [[CrossRef](#)]
2. Shoreh, A.A.-H.; Kuznetsov, N.V.; Mokaev, T.N. New adaptive synchronization algorithm for a general class of complex hyperchaotic systems with unknown parameters and its application to secure communication. *Phys. A* **2022**, *586*, 126466.
3. Nagamani, G.; Soundararajan, G.; Subramaniam, R.; Azeem, M. Robust extended dissipativity analysis for Markovian jump discrete-time delayed stochastic singular neural networks. *Neural Comput. Appl.* **2020**, *32*, 9699–9712. [[CrossRef](#)]
4. Radhika, T.; Nagamani, G.; Zhu, Q.X.; Ramasamy, S.; Saravanakumar, R. Further results on dissipativity analysis for Markovian jump neural networks with randomly occurring uncertainties and leakage delays. *Neural Comput. Appl.* **2018**, *30*, 3565–3579. [[CrossRef](#)]
5. Zhou, C.; Wang, C.H.; Yao, W.; Lin, H.R. Observer-based synchronization of memristive neural networks under DoS attacks and actuator saturation and its application to image encryption. *Appl. Math. Comput.* **2022**, *425*, 127080.
6. Shi, K.B.; Cai, X.; She, K.; Wen, S.P.; Zhong, S.M.; Park, P.; Kwon, O.-M. Stability analysis and security-based event-triggered mechanism design for T-S fuzzy NCS with traffic congestion via DoS attack and its application. *IEEE Trans. Fuzzy Syst.* **2023**, *31*, 3639–3651. [[CrossRef](#)]
7. Reyhanoglu, M.; Jafari, M. A simple learning approach for robust tracking control of a class of dynamical systems. *Electronics* **2023**, *12*, 2026. [[CrossRef](#)]
8. Ding, K.; Zhu, Q.X. A note on sampled-data synchronization of memristor networks subject to actuator failures and two different activations. *IEEE Trans. Circuits Syst. II Express Briefs* **2021**, *68*, 2097–2101.
9. Yang, X.T.; Wang, H.; Zhu, Q.X. Event-triggered predictive control of nonlinear stochastic systems with output delay. *Automatica* **2022**, *140*, 110230.
10. Kumar, L.; Dhillon, S.S. Tracking control design for fractional order systems: A passivity-based port-Hamiltonian framework. *ISA Trans.* **2023**, *138*, 1–9. [[CrossRef](#)]

11. Tang, R.Q.; Su, H.S.; Zou, Y.; Yang, X.S. Finite-time synchronization of markovian coupled neural networks with delays via intermittent quantized control: Linear programming approach. *IEEE Trans. Neural Netw. Learn. Syst.* **2021**, *33*, 5268–5278. [[CrossRef](#)]
12. Stamova, I.; Stamov, G. Mittag-Leffler synchronization of fractional neural networks with time-varying delays and reaction-diffusion terms using impulsive and linear controllers. *Neural Netw.* **2017**, *96*, 22–32. [[PubMed](#)]
13. Stamov, G.; Stamova, I. Extended stability and control strategies for impulsive and fractional neural networks: A review of the recent results. *Fractal Fract.* **2023**, *7*, 289.
14. Tang, Y.; Zhou, L.; Tang, J.H.; Rao, Y.; Fan, H.G.; Zhu, J.H. Hybrid impulsive pinning control for mean square synchronization of uncertain multi-link complex networks with stochastic characteristics and hybrid delays. *Mathematics* **2023**, *11*, 1697. [[CrossRef](#)]
15. Deng, L.P.; Wu, Z.Y. Impulsive cluster synchronization in community network with nonidentical nodes. *Commun. Theor. Phys.* **2012**, *58*, 525–530. [[CrossRef](#)]
16. Peng, D.X.; Li, X.D. Leader-following synchronization of complex dynamic networks via event-triggered impulsive control. *Neurocomputing* **2020**, *412*, 1–10. [[CrossRef](#)]
17. Yang, X.; Lu, J.; Ho, D.W.C.; Song, Q. Synchronization of uncertain hybrid switching and impulsive complex networks. *Appl. Math. Model.* **2018**, *59*, 379–392. [[CrossRef](#)]
18. Fan, H.G.; Shi, K.B.; Zhao, Y. Pinning impulsive cluster synchronization of uncertain complex dynamical networks with multiple time-varying delays and impulsive effects. *Phys. A* **2022**, *587*, 126534. [[CrossRef](#)]
19. Kchaou, M.; Tadeo, F.; Chaabane, M.; Toumi, A. Delay-dependent robust observer-based control for discrete-time uncertain singular systems with interval time-varying state delay. *Int. J. Control Autom. Syst.* **2014**, *12*, 12–22. [[CrossRef](#)]
20. Kchaou, M.; Mahmoud, M.S. Robust  $(Q, S, R)$ - $\gamma$ -dissipative sliding mode control for uncertain discrete-time descriptor systems with time-varying delay. *IMA J. Math. Control Inf.* **2018**, *35*, 735–756. [[CrossRef](#)]
21. Li, H.L.; Cao, J.D.; Hu, C.; Zhang, L.; Wang, Z.L. Global synchronization between two fractional-order complex networks with non-delayed and delayed coupling via hybrid impulsive control. *Neurocomputing* **2019**, *356*, 31–39.
22. Yang, X.S.; Li, X.D.; Lu, J.Q.; Cheng, Z.S. Synchronization of time-delayed complex networks with switching topology via hybrid actuator fault and impulsive effects control. *IEEE Trans. Cybern.* **2020**, *50*, 4043–4052. [[CrossRef](#)] [[PubMed](#)]
23. Feng, J.W.; Yu, F.F.; Zhao, Y. Exponential synchronization of nonlinearly coupled complex networks with hybrid time-varying delays via impulsive control. *Nonlinear Dyn.* **2016**, *85*, 621–632.
24. Zhang, L.; Yang, X.S.; Xu, C.; Feng, J.W. Exponential synchronization of complex-valued complex networks with time-varying delays and stochastic perturbations via time-delayed impulsive control. *Appl. Math. Comput.* **2017**, *306*, 22–30.
25. Ye, J.R.; Zhang, J.E. Delayed impulsive control for lag synchronization of neural networks with time-varying delays and partial unmeasured states. *Discret. Dyn. Nat. Soc.* **2022**, *2022*, 9308923. [[CrossRef](#)]
26. Liu, X.Z.; Zhang, K.X. Synchronization of linear dynamical networks on time scales: Pinning control via delayed impulses. *Automatica* **2016**, *72*, 147–152. [[CrossRef](#)]
27. Yang, X.S.; Yang, Z.C. Synchronization of TS fuzzy complex dynamical networks with time-varying impulsive delays and stochastic effects. *Fuzzy Sets Syst.* **2014**, *235*, 25–43.
28. Wu, T.; Xiong, L.L.; Cao, J.D.; Park, J.H.; Cheng, J. Synchronization of coupled reaction-diffusion stochastic neural networks with time-varying delay via delay-dependent impulsive pinning control algorithm. *Commun. Nonlinear Sci. Numer. Simul.* **2021**, *99*, 105777. [[CrossRef](#)]
29. Li, X.D.; Song, S.J.; Wu, J.H. Exponential stability of nonlinear systems with delayed impulses and applications. *IEEE Trans. Autom. Control* **2019**, *64*, 4024–4034. [[CrossRef](#)]
30. Stamoval, I. Global Mittag-Leffler stability and synchronization of impulsive fractional-order neural networks with time-varying delays. *Nonlinear Dyn.* **2014**, *77*, 1251–1260.
31. Chen, T.P.; Wang, L.L. Global  $\mu$ -stability of delayed neural networks with unbounded time-varying delays. *IEEE Trans. Neural Netw.* **2007**, *18*, 1836–1840. [[CrossRef](#)]
32. Fan, H.G.; Xiao, Y.; Shi, K.B.; Wen, H.; Zhao, Y.  $\mu$ -synchronization of coupled neural networks with hybrid delayed and non-delayed impulsive effects. *Chaos Solitons Fractals* **2023**, *173*, 113620. [[CrossRef](#)]
33. Cui, H.M.; Guo, J.; Feng, J.X.; Wang, T.F. Global  $\mu$ -stability of impulsive reaction-diffusion neural networks with unbounded time-varying delays and bounded continuously distributed delays. *Neurocomputing* **2015**, *157*, 1–10.
34. Liu, X.W.; Chen, T.P. Robust  $\mu$ -stability for uncertain stochastic neural networks with unbounded time-varying delays. *Phys. A* **2008**, *387*, 2952–2962. [[CrossRef](#)]
35. Chen, T.P.; Wu, W.; Zhou, W.J. Global  $\mu$ -synchronization of linearly coupled unbounded time-varying delayed neural networks with unbounded delayed coupling. *IEEE Trans. Neural Netw.* **2008**, *19*, 1809–1816. [[CrossRef](#)] [[PubMed](#)]
36. Xu, Z.L.; Li, X.D.; Duan, P.Y. Synchronization of complex networks with time-varying delay of unknown bound via delayed impulsive control. *Neural Netw.* **2020**, *125*, 224–232. [[PubMed](#)]
37. Huang, Y.L.; Qiu, S.H.; Ren, S.Y.; Zheng, Z.W. Fixed-time synchronization of coupled Cohen-Grossberg neural networks with and without parameter uncertainties. *Neurocomputing* **2018**, *315*, 157–168.
38. Kaviarasan, B.; Sakthivel, R.; Lim, Y. Synchronization of complex dynamical networks with uncertain inner coupling and successive delays based on passivity theory. *Neurocomputing* **2016**, *186*, 127–138.

39. Wang, G.; Lu, S.W.; Liu, W.B.; Ma, R.N. Adaptive complete synchronization of two complex networks with uncertain parameters, structures, and disturbances. *J. Comput. Sci.* **2021**, *54*, 101436. [[CrossRef](#)]
40. Narayanan, G.; Ali, M.S.; Alsulami, H.; Stamov, G.; Stamova, I.; Ahmad, B. Impulsive security control for fractional-order delayed multi-agent systems with uncertain parameters and switching topology under DoS attack. *Inf. Sci.* **2022**, *618*, 169–190.
41. Wang, Y.Q.; Lu, J.Q.; Li, X.D.; Liang, J.L. Synchronization of coupled neural networks under mixed impulsive effects: A novel delay inequality approach. *Neural Netw.* **2020**, *127*, 38–46. [[PubMed](#)]

**Disclaimer/Publisher's Note:** The statements, opinions and data contained in all publications are solely those of the individual author(s) and contributor(s) and not of MDPI and/or the editor(s). MDPI and/or the editor(s) disclaim responsibility for any injury to people or property resulting from any ideas, methods, instructions or products referred to in the content.